

# Spatially distributed potential evapotranspiration modelling and climate projections

Salem S. Gharbia<sup>1,\*</sup>, Trevor Smullen<sup>1</sup>, Laurence Gill<sup>2</sup>, Paul Johnston<sup>2</sup>, and

Francesco Pilla<sup>1</sup>

<sup>1</sup> *Department of Planning and Environmental Policy, University College Dublin (UCD),  
Dublin, Ireland.*

<sup>2</sup> *Department of Civil, Structural and Environmental Engineering, Trinity College, Dublin,  
Ireland.*

---

## Abstract

Evapotranspiration integrates energy and mass transfer between the Earth's surface and atmosphere and is the most active mechanism linking the atmosphere, hydrosphere, lithosphere and biosphere. This study focuses on the fine resolution modelling and projection of spatially distributed potential evapotranspiration on the large catchment scale as response to climate change. Six potential evapotranspiration designed algorithms, systematically selected based on a structured criteria and data availability, have been applied and then validated to long-term mean monthly data for the Shannon River catchment with a 50 m<sup>2</sup> cell size. The best validated algorithm was therefore applied to evaluate the possible effect of future climate change on potential evapotranspiration rates. Spatially distributed potential evapotranspiration projections have been modeled based on climate change projections from multi-GCM ensembles for three future time intervals (2020, 2050 and 2080) using a range of different Representative Concentration Pathways producing four scenarios for each time interval. Finally, seasonal results have been compared to baseline results to evaluate the impact of climate change on the potential evapotranspiration and therefor on the catchment dynamical water

---

\* Corresponding author. Tel.: +353899808313.  
E-mail address: salem.gharbia@ucd.ie

25 balance. The results present evidence that the modeled climate change scenarios would have a significant  
26 impact on the future potential evapotranspiration rates. All the simulated scenarios predicted an increase in  
27 potential evapotranspiration for each modeled future time interval, which would significantly affect the  
28 dynamical catchment water balance. This study addresses the gap in the literature of using GIS-based  
29 algorithms to model fine-scale spatially distributed potential evapotranspiration on the large  
30 catchment systems based on climatological observations and simulations in different climatological  
31 zones. Providing fine-scale potential evapotranspiration data is very crucial to assess the dynamical  
32 catchment water balance to setup management scenarios for the water abstractions. This study  
33 illustrates a transferable systematic method to design GIS-based algorithms to simulate spatially distributed  
34 potential evapotranspiration on the large catchment systems.

35

36 *Keywords:* GIS; Evapotranspiration; Geospatial-statistical; Algorithm.

---

37

38

40 After precipitation, evapotranspiration is the largest component of the terrestrial hydrological budget  
41 and thus critical for water resources evaluation and sustainable water management policies (Liu and  
42 Phinn, 2003, Portugali et al., 1994, Wu, 2002). Evapotranspiration is responsible for transferring  
43 moisture from the earth's surface to the atmosphere in vapor form. Due to complex interactions  
44 between meteorological and site-specific factors, evapotranspiration is extremely difficult to quantify.  
45 Water balance modeling requires the spatial estimation of potential evapotranspiration (PETS)  
46 throughout the catchment; that is the evapotranspiration, which would occur under optimal  
47 conditions. Evapotranspiration includes two processes that occur simultaneously in the soil-plant-  
48 atmosphere system, direct evaporation of moisture from the Earth's surface, and the exchange of  
49 water vapor, which occurs within the leaves of plants (transpiration) (Swenson and Wahr, 2006,  
50 Wilson et al., 2001). Evapotranspiration has long been recognized as a central process in the  
51 hydrological cycle (Penman, 1948, Rosenzweig, 1968, Holdridge, 1959, Gordon, 1998). The term  
52 potential evapotranspiration represents the ET, which would occur under optimal conditions where  
53 evapotranspiration is not limited by factors such as soil moisture. Evapotranspiration represents the  
54 most active of land-based hydrological processes, with approximately 65% of precipitation being  
55 evaporated and transpired (Kite and Droogers, 2000, Shukla and Mintz, 1982). Evapotranspiration  
56 fulfills numerous roles throughout its cycle. It accomplishes energy (heat) and mass (water  
57 vapor) transfer between the Earth's surface and atmosphere, and is the most active mechanism  
58 connecting the atmosphere, hydrosphere, lithosphere and biosphere (Zhao et al., 2004, Kite and  
59 Droogers, 2000, Zhang et al., 2001). Evapotranspiration is not only responsible for modulating  
60 atmospheric moisture but also temperature. Therefore, it can be seen that this process provides a vital  
61 link between the climatic, hydrological and ecological systems. Potential evapotranspiration remains  
62 one of the least satisfactorily explained processes in the hydrological cycle, principally because of its  
63 spatial variability (Andréassian, 2004, Andréassian et al., 2004, Oudin et al., 2005).

64 Due to the complexity and difficulties faced in the measurement of PETS, it is predominately  
65 estimated using formulae and observed meteorological data. There exists a vast number of models for

66 estimating PETS, which may be grouped into several categories such as radiation, water budget, mass  
67 transfer, temperature, and combination methods. These methods vary greatly in terms of complexity,  
68 data requirements, and reliability.

69 Developing a GIS tool for modeling spatially distributed PETS from an undefined number of  
70 meteorological stations from monthly data of precipitation and temperature is the main objective of  
71 this paper. This tool provides the user with the PETS results on a seasonal and annual basis as well  
72 as an option to calculate values on a monthly frequency. The PETS GIS tool is presented using many  
73 methods with the ability to calibrate and validate the results. This study presents the primary results  
74 of the calculated PETS for both the baseline period and the future periods, based on climate change  
75 projections, for the Shannon River catchment in Ireland (Gharbia et al., 2016d, Gharbia et al., 2016b,  
76 Gharbia et al., 2015b, Gharbia et al., 2016a, Gharbia et al., 2015a). The River Shannon catchment,  
77 the focus of this study, is the largest transboundary river system and catchment in the island of  
78 Ireland and one of the most important water and power resources in the Republic of Ireland, see  
79 Figure 1. Met Éireann, the Irish National Meteorological Service, calculates daily estimates of PETS  
80 at 25 synoptic weather stations throughout Ireland using the FAO Penman-Monteith method, 4 of  
81 which are located within the Shannon River catchment. As the catchment covers in excess of 18 000  
82 km<sup>2</sup>, it is evident that 4-point estimates are not sufficient to estimate spatially distributed PETS. The  
83 Penman-Monteith method is widely considered as a standard method for the calculation of PETS.  
84 However, its application, particularly for this large catchment, is questionable due to the need for  
85 specific data for a variety of parameters, which are only available from a limited number of locations  
86 and will result in interpolation of data from distant meteorological stations. As a result, less data  
87 intensive empirical models are often utilized which allows for data from a greater number of  
88 meteorological stations to be used thus resulting in more spatially representative estimates. This  
89 study is addressing the gap in the literature of using GIS-based algorithms to calculate the fine scale  
90 spatially distributed PETS on the large catchment systems based on climatological observations and  
91 simulations.



94

## *Materials and Methods*

### Evaluating and choosing models to quantify PETS

96 The reliability of PETS estimates depends upon the number of stations from which data is obtained  
97 and the number of years of available data (Chattopadhyay and Hulme, 1997), as more stations gives  
98 more accurate spatially distributed PETS, based on the used spatial interpolation method the  
99 minimum number of needed stations can statistically be calculated which is not available in reality in  
100 most of the cases. As a result, numerous authors such as (Xu and Singh, 2002, Fennessey and Vogel,  
101 1996, Chattopadhyay and Hulme, 1997, Oudin et al., 2005, Kite and Droogers, 2000) among many  
102 others, recommend that more simplified methods be used when only a limited number of  
103 meteorological stations are available with the required data.

104 Studies have focused on developing methods to accurately estimate PETS and improve on existing  
105 methods for over 70 years. In that time, numerous studies of varying scope have been completed to  
106 determine the most suitable model to be used to estimate PETS for varying purposes. (Jensen et  
107 al., 1990) evaluated 20 formulae for estimating PETS versus lysimeter data from around the world.  
108 He concluded that the Penman-Monteith method was the best method, while the performance of the  
109 remainder varied depending on calibration and local conditions. As discussed previously, methods are  
110 most suited to the environment in which they were developed.

111 In evaluating models to estimate PETS it is also necessary to consider what the requirements are for  
112 the calculated values. For instance, (Oudin et al., 2005) compared the performance of 27 PETS  
113 models over 308 catchments to find the most relevant for rainfall-runoff models. It was found that  
114 temperature and radiation based methods performed best and are as efficient as models that are far  
115 more complex. Kay and Davies (2008) investigated the performance of a simple temperature based  
116 formula proposed by (Oudin et al., 2005) compared to that of the Penman-Monteith method. PETS  
117 estimates using both methods were compared to that of the UK meteorological office's PETS values  
118 for a 30-year period 1961-1990. It was found that the much simpler temperature based method  
119 generally gave better estimates of PETS than the Penman-Monteith method. This supports the opinion

120 of many authors who consider more simple models, once locally calibrated, to be as effective as more  
121 complex models (Xu and Singh, 2002, Fennessey and Vogel, 1996, Chattopadhyay and Hulme, 1997,  
122 Oudin et al., 2005, Kite and Droogers, 2000).

123 CGIAR-CSI (2007) spatially estimated PETS using 4 temperature-based models (Droogers and  
124 Allen, 2002, Hargreaves and Samani, 1985, Holland, 1978, Thornthwaite, 1948). The results for  
125 each were compared to PETS values at 2288 meteorological stations in South America and South  
126 Africa. Based on the results, the Hargreaves & Samani method was chosen as the most suitable to  
127 model PETS globally. The Hargreaves model was found to perform almost as well the Penman-  
128 Monteith method but required far less parameterisation with significantly less sensitivity to error in  
129 climate inputs.

130 The most comprehensive research on available PETS formulae has been completed by Xu and Singh  
131 who commenced a research program in 1996. Their first paper investigated thirteen equations based  
132 on the mass-transfer method; these equations were expressed in seven generalised equations  
133 (Singh and Xu, 1997). The seven generalized equations were then compared with pan evaporation  
134 results at four climatological stations in north-western Ontario, Canada. All of the formulae yielded  
135 satisfactory estimates for monthly PETS. As discussed previously, model parameters were required to  
136 be calibrated using local meteorological variables.

137 Xu and Singh (2000) then evaluated five radiation based PETS formulae (Abtew, Hargreaves,  
138 Makkink, Priestley-Taylor and Turc), which were compared with pan evaporation measured at  
139 Changing station in Switzerland (Turc, 1961, De Bruin, 1983, Makkink, 1957, Hargreaves and  
140 Samani, 1982, Abtew, 1996, Xu and Singh, 2000). The evaluation and comparison process were first  
141 completed using original empirical constants and then using recalibrated constant values. Using  
142 original values, the Abtew formula was found to give reasonable estimates of PETS while the  
143 remainder demonstrated large errors. With recalibrated constants, a significant improvement was  
144 found in four out of the five methods. The Makkink and Priestley-Taylor formulae were concluded  
145 to be the best methods for use in the study region. Xu and Singh (2001) also evaluated and compared  
146 seven temperature-based formulae (Thornthwaite, Linacre, Blaney-Criddle, Hargreaves, Kharrufa,

147 Hamon, Romanenko) with data from two climatological stations (Rawson Lake and Atikokan) in  
148 north-western Ontario, Canada. Similar to the foregoing study comparisons were made using both  
149 original and recalibrated constant values (Romanenko, 1973, Hamon, 1961, Kharrufa, 1985, Blaney  
150 and Criddle, 1964, Linacre, 1977, Xu and Singh, 2001, Hargreaves and Samani, 1982, Thornthwaite,  
151 1948). Using original constants, the Blaney-Criddle equation resulted in mean seasonal evaporation  
152 values that agreed most closely with pan evaporation values, while the remainder demonstrated large  
153 errors. With recalibrated constant values, all seven methods provided reasonable results. With  
154 properly determined constant values, the Blaney–Criddle, Hargreaves and Thornthwaite methods were  
155 concluded to be the best temperature based methods for the study area. Based on the results of the  
156 foregoing studies Xu and Singh (2002) selected the best methods from each of the three categories:  
157 (i) mass-transfer based methods, (ii) radiation based methods, and (iii) temperature-based methods. A  
158 cross comparison of the best formulae selected from each category was made. Five PETS formulae  
159 (Hargreaves and Blaney-Criddle (temperature-based), Makkink and Priestley-Taylor (radiation-  
160 based) and Rohwer (mass-transfer-based)) were evaluated and compared with PETS values calculated  
161 using the Penman-Monteith method using daily meteorological data from the Changing station in  
162 Switzerland for the 5-year period 1990-1994. The calculations of the Penman-Monteith equation  
163 followed the procedure recommended by FAO (Allen, 2000). Both original and recalibrated constant  
164 values were used. With original constant values, all except the Blaney-Criddle method returned  
165 reasonably similar results to the Penman-Monteith method. Significant improvement was achieved for  
166 the Blaney-Criddle method by recalibrating constants and adding a transition period in determining  
167 the parameter k. Constant values were also recalibrated for the remaining methods. It was concluded  
168 from the study that, using locally determined parameter values, all five empirical methods gave  
169 acceptable estimates of PETS. The methods were ranked as follows:

- 170 1. Priestley-Taylor (Radiation-based).
- 171 2. Makkink (Radiation-based).
- 172 3. Hargreaves (temperature-based).
- 173 4. Blaney-Criddle (temperature-based).

174 5. Rohwer (Mass-transfer).

175 6. Penman-Monteith.

176 This ranking gives a very useful insight of which method can be recommended to be used in  
177 calculating evapotranspiration based on the data availability. It was also concluded that the  
178 differences in performance between the best methods selected from each category are smaller than  
179 the differences between the different methods within each category as reported in earlier studies.

180 As mentioned, empirical PETS formulae are typically developed using site-specific data and  
181 experiments, thus their performance will vary depending on location and local conditions. Although  
182 calibration of empirical constants with local data will maximize a given formula's performance for  
183 local conditions, the performance relative to other methods will continue to vary. Therefore, from the  
184 aforementioned comparative studies, all of which were completed outside of Ireland, it is not possible  
185 to identify the method most suited for use in Irish conditions. It is possible to identify the continuously  
186 best-performing methods and those which would be best suited for use in this study.

187 From a review of available literature, eight PETS models were selected, as listed in Table 1. These  
188 methods were selected as they are the generally best performing methods and those which are most  
189 suited to spatially estimate PETS within a GIS platform.

190 In order to further evaluate the chosen methods, four criteria were chosen by which to evaluate their  
191 suitability. Under each of the criteria, each method receives a rating between 1 and 3. The three  
192 methods with the lowest cumulative rating will be selected for further evaluation with local data and  
193 subject to the data availability.

194 The evaluation criteria were as follows:

195 A. The number of climatological datasets required e.g. Temperature, wind speed etc. Ratings for  
196 this criterion are as follows: 1 dataset = 1; 2 datasets = 2; 3+ datasets = 3.

197 B. The spatial availability of required data. Ratings for this criterion are as follows: temperature,  
198 precipitation = 1; wind speed = 2; Radiation, vapour pressure, atmospheric pressure = 3.

199 C. The number of computations required, which can be illustrated by the amount of map algebra  
 200 functions that needed to complete the PETS calculation for a single pixel of the catchment  
 201 within the GIS environment. The complexity of available empirical PETS models varies  
 202 greatly from relatively simple methods requiring an evaluation of a single formula to those,  
 203 which would require an evaluation of several formulae prior to application of a formula to  
 204 estimate PETS. Ratings for this criterion are as follows: 1 computation = 1; 2 computations  
 205 = 2; 3+ computations = 3.

206 D. Suitability for use within a GIS platform. Ratings for this criterion are as follows: Easily  
 207 applied = 1; moderate = 2; difficult to apply = 3

208 **Table 1: PETS models rating. (A) number of climatological datasets required. (B) the**  
 209 **spatial availability of required data. (C) the number of computations required. (D)**  
 210 **Suitability for use within a GIS platform. (Total) the cumulative rating.**

Method	Category	(A)	(B)	(C)	(D)	(Total)
<b>Priestley-Taylor</b>	Radiation	3	3	2	3	11
<b>Makkink</b>	Radiation	3	3	1	3	10
<b>Hargreaves &amp; Samni</b>	Temperature	1	1	2	1	5
<b>Blaney Criddle</b>	Temperature	1	1	1	1	4
<b>Hargreaves</b>	Temperature	1	1	2	1	5
<b>Thornwhite</b>	Temperature	1	1	3	2	7
<b>Linacre</b>	Temperature	1	1	1	1	4
<b>Rohwer</b>	Mass Transfer	3	3	1	1	8
<b>Penman-Monteith</b>	Mass Transfer	3	3	3	3	12

211 From the application of the rating procedure, four PETS models were identified as being the most  
 212 suitable (Hargreaves & Samani, Blaney-Criddle, Hargreaves, Linacre), which were taken to further  
 213 assessment regarding the data availability and the suitability for the study area.

214 In order to run the PETS simulation using the evaluated methods, it was the intention to use lysimeter

215 data from a trusted device, lysimeter that has been continuously validated by the water budget  
216 equation, to calibrate the chosen empirical equations for local conditions. Whilst reviewing the data  
217 sources in Ireland, it was found that three lysimeters were operated by Met Éireann, as reported on  
218 Met Éireann's website. However, it transpired that only one lysimeter is maintained by Met Éireann,  
219 which is located on Valentia Island. Due to its location on a small island in the Atlantic Ocean data  
220 from the lysimeter would not be representative of the Shannon River Basin District. The remaining  
221 two locations were found to be operated by Teagasc, The Agriculture and Food Development  
222 Authority, and we could not access this data.

223 Because of the absence of reliable PETS data with which those evaluated methods previously  
224 shortlisted may be calibrated it was not possible to calibrate nor identify the most appropriate method  
225 for use within the Shannon River Basin District. As it was not possible to recalibrate the selected  
226 models for local conditions and thus identify the best performing model for application within the  
227 GIS, a number of models were selected for the application. In order to evaluate the performance  
228 of the model, short-term monthly data was sourced from Met Éireann. This data consisted of  
229 mean monthly values of PETS for four synoptic weather stations within the Shannon, the PETS  
230 values were calculated by Met Éireann by Penman-Monteith using the full range of required input  
231 data for the four-point locations, this data was compared with the calculated results from PETS  
232 models as an evaluation step.

233 As discussed previously, because of the absence of lysimeter PETS data it was not possible to  
234 complete a comparative recalibration of the PETS models shortlisted. This study aimed to produce  
235 a GIS tool to simulate PETS using different simulation methods, this tool used six methods for  
236 spatially distributed PETS modeling as follow:

237

- 238 • **Blaney-Criddle (Allen and Pruitt, 1986).**

239 The Blaney-Criddle (1950) method for estimating PETS is most well known in the U.S.A, but it has  
240 been used extensively elsewhere. For example, the FAO temperature methodology recommended by

241 (Pruitt and Doorenbos, 1977) is based on the Blaney-Criddle method. Although initially used for  
242 estimating the consumptive use of irrigated crops in the western United States, it is uniformly  
243 applicable for estimating PETS in agricultural lands or catchments with reasonably uniform  
244 vegetation. The common form of the Blaney-Criddle equation is:

$$\text{PETS} = K_p(0.46 T_A + 8.13) \quad \text{Eq 1}$$

245  
246 where PETS is evapotranspiration in mm from a reference crop for the period in which p is  
247 expressed,  $T_a$  is the mean temperature in °C for the same period, p represents the percentage of total  
248 daytime hours for the period used (whether daily, weekly, monthly etc.) out of total daytime  
249 hours of the year, i.e. 365x12, and k is a monthly consumptive use coefficient (Pruitt and Doorenbos,  
250 1977), depending on vegetation type, location and season.

251 Blaney-Criddle recognized that temperature has one of the greatest influences on ET rates and that  
252 records are far more uniformly available than other factors. Furthermore, sunshine hours were also  
253 identified as a noteworthy factor in the rate at which plants grow and consume water. However,  
254 sunshine records are not usually available thus Blaney-Criddle recommended the use of tables of  
255 theoretical sunshine hours for different latitudes in the absence of actual data.

256

257 • **Kharrufa (Kharrufa, 1985).**

258 Kharrufa (1985) derived a relatively simple equation similar to that of Blaney-Criddle described  
259 previously with which PETS may be calculated. PETS is calculated based on a relationship between  
260 temperature and sunshine duration and is given by:

$$\text{PETS} = 0.34 P T_A^{1.3} \quad \text{Eq 2}$$

262 where PETS is evapotranspiration in mm/month and p and  $T_a$  has the same definitions as that given  
263 previously.

264

265 • **Hargreaves and Samani (Hargreaves and Samani, 1982).**

266 Hargreaves (1975) published an empirical equation for estimating PETS which was developed using  
267 data from a precision lysimeter and weather data for an 8-year period. It was found for a 5-day time  
268 step that 94% of the variance in measured versus modeled values was explained through average  
269 temperature and solar radiation. The portion of extra-terrestrial solar radiation which penetrates  
270 through clouds and reaches the earth's surface is the primary heat source for ET processes.  
271 Subsequent studies by Hargreaves and Samani (1982) showed solar radiation may be estimated from  
272 the difference between maximum and minimum temperature (Hargreaves and Samani, 1982). This is  
273 possible as under clear skies incoming solar radiation may pass freely through the atmosphere  
274 resulting in high temperatures while at night temperatures are low due to outgoing longwave radiation  
275 (Allen et al., 1998). Contrastingly under cloudy conditions a fraction of the incoming solar  
276 radiation is prevented from reaching earth thus resulting in lower temperatures, while at night  
277 temperatures are higher as cloud cover limits outgoing longwave radiation. As solar radiation data is  
278 frequently unavailable Hargreaves and Samani recommended estimating it from extra-terrestrial  
279 radiation and minimum and maximum temperature. Based on their previous studies Hargreaves and  
280 Samani (1985) presented a simplified equation, w h i c h requires only temperature, the day of the  
281 year and latitude.

282

$$283 \text{ PETS} = 0.0135 K_{RS} (RA / \lambda) (T_{\max} - T_{\min})^{0.5} * (T_A + 17.8) \quad \text{Eq 3}$$

284

285 where PETS is the monthly evapotranspiration rate in mm,  $K_{RS}$  is an empirical radiation  
286 adjustment coefficient,  $\lambda$  is the latent heat of vaporization in MJ/kg, for the mean air temperature  
287 commonly assumed to equal 2.45 MJ/kg, RA is the extra-terrestrial solar radiation in  
288 MJ/m<sup>2</sup>/month.  $T_{\max}$  and  $T_{\min}$  are monthly maximum and minimum monthly temperature in °C,  
289 the constant 0.0135 is a factor to convert from empirical US units to the international system of metric  
290 units.  $T_A$  is the mean temperature in °C.

291

292 • **Oudin (Oudin et al., 2010).**

293 (Oudin et al., 2005) examined the efficiency of 27 PETS models over a large sample of 308  
294 catchments which were located in France, Australia, and the USA. It was found that models based  
295 upon temperature and solar radiation performed best. Oudin selected two of the best performing  
296 models (Jensen-Haise and McGuinness) both of which had the same generalized form (Parmele and  
297 McGuinness, 1974, McGuinness and Bordne, 1972). Oudin then calibrated his formula over the  
298 catchments and produced a common formula given by:

$$299 \text{ PETS} = \frac{RA}{\lambda \rho} \frac{T_a}{100} \quad \text{Eq 4}$$

300 where PETS is monthly potential evapotranspiration in mm and  $\rho$  is the relative density of water  
301 which = 1,  $\lambda$  is the latent heat of vaporization in MJ/kg, RA is the extra-terrestrial solar radiation in  
302 MJ/m<sup>2</sup>/month, T<sub>a</sub> is the mean temperature in °C.

303 The equation relies on expected solar radiation as calculated from Julian day and latitude and not  
304 actual measured data; thus, the only real independent variable is temperature. Therefore, the Oudin  
305 equation, similar to the Hargreaves and Samani method discussed previously, is referred to as a  
306 temperature based method although it has a strong dependency on solar radiation.

307

308 • **Thornthwaite (Thornthwaite and Mather, 1957)**

309 Thornthwaite (1948) developed a methodology to estimate evapotranspiration for short vegetation.  
310 This is a widely used method which was derived by correlating values of mean monthly temperature  
311 with that of evapotranspiration for valleys where sufficient soil moisture was always available to  
312 sustain active transpiration (Thornthwaite, 1948). The Thornthwaite method determines values of  
313 PETS using values of observed air temperature and duration of sunlight data, the rationale being that  
314 air temperature acts as a proxy to net radiation. The determination of monthly PETS involves a  
315 number of computational steps as follows:

$$316 \text{ PETS}' = C \left( \frac{10T_a}{I} \right)^a \quad \text{Eq 5}$$

317 where PETS' is the unadjusted monthly potential evapotranspiration in mm, C is a constant = 16, I is  
318 the annual heat index given by equation 7, and  $a$  is an empirical exponent given by equation 7.8. The

319 annual value of the heat index  $I$  is calculated by summing monthly indices over a 12-month period.

320 The monthly indices are obtained from the equation:

$$321 \quad i = \frac{T_a^{1.51}}{5} \quad \text{Eq 6}$$

322 The yearly heat index is calculated by:

$$323 \quad I = \sum_1^{12} i_j \quad \text{Eq 7}$$

324 The exponent  $a$  is calculated by:

$$325 \quad a = (67.5 \times 10^{-8} I^3) - (77.1 \times 10^{-6} I^2) + (0.0179 I) + 0.492 \quad \text{Eq 8}$$

326

327 PETS' which is calculated using equation 5 is an unadjusted monthly value of PETS for a standard  
328 month with 30 days with 12 hr/day of sunlight. These PETS' values were adjusted depending on the  
329 number of days in a month and the duration of average monthly daylight which is a function of season  
330 and latitude. This process for any month is given by:

$$331 \quad \text{PETS} = \text{PET}' \frac{d}{12} \left( \frac{N}{30} \right) \quad \text{Eq 9}$$

332 where PETS is the adjusted monthly potential evapotranspiration in mm,  $d$  is the duration of average  
333 monthly daylight in hours, and  $N$  is the number of days in a given month (1 – 31 days).

334

335 **• Hamon (Hamon, 1961)**

336 Hamon (1961) formulated a simplified expression to estimate PETS. The method proposed by  
337 Hamon is most commonly used for monthly, seasonally or yearly estimates of PETS. The Hamon  
338 method estimates PETS given mean air temperature and day length data. The Hamon method has  
339 been employed globally for hydrological studies where only temperature data is available (Hamon,  
340 1961). The simplified equation proposed by Hamon is given by:

$$341 \quad \text{PETS} = 0.55 D^2 P_t \quad \text{Eq 10}$$

342 where PETS is the monthly potential evapotranspiration in mm,  $D$  is the hours of daylight for a given  
343 month in units of 12hr [hr/12hr] and  $P_t$  is a saturated water vapor density term calculated by:

344 
$$Pt = \frac{4.95 e^{0.062Ta}}{100}$$
 Eq 11

345 This method was developed based on the relationship between PETS, maximum possible radiant  
346 energy and moisture-holding capacity of the air at the prevailing air temperature. Hamon determined  
347 the constant value of 0.55 through comparison of results from the far more complex Thornthwaite  
348 method discussed previously. Sunlight hours are used as a proxy for incoming radiant energy while Pt  
349 is used as a proxy for moisture-holding capacity of the air. It's worth mentioning that Solar Radiation  
350 would be a better representation of both daylight and sunlight hours as solar radiation considers the  
351 cloud covers, however the Hamon method got developed, calibrated and validated using the daylight  
352 and sunlight hours parameters which helps in the cases of not availability of solar radiation data.  
353 Redeveloping Hamon method using solar radiation parameter would be a very interesting future  
354 research topic.

355

## 356 Data Setup

357 In this paper, the required data is mainly climatological data for the baseline and four future scenarios.  
358 Multi-dimensional datasets for temperature, humidity, windspeed, precipitation and solar radiation, all  
359 with minimum, mean and maximum values, for the Shannon River catchment were obtained from  
360 (Gharbia et al., 2016b, Gharbia et al., 2016c). Climate change projections for the Shannon River  
361 Basin District were obtained for several climate variables from Gharbia et al. (2016b), including  
362 mean monthly temperature, from multi-GCM ensembles for three future time intervals (2020, 2050  
363 and 2080) using a range of different Representative Concentration Pathways (RCPs). The climate  
364 change models were based upon two different RCPs; using a radiative forcing of 4.5 W/m<sup>2</sup> and 8.5  
365 W/m<sup>2</sup> respectively, which were produced from 50% (median) and 75% (3rd quartile) multi-GCM  
366 ensembles results.

367 In general, Gharbia et al. (2016b) simulations results show that temperature will increase every year,  
368 in particular RCP 8.5 (75%) has the highest increasing rate (1.85°C in 2080 as an average over  
369 Shannon catchment), which is consistent with the global rise in air temperatures. Gharbia et al.

370 (2016b) concluded that all seasons would have an increase in temperature with the highest increases  
371 occurring in the spring and summer. Trends in precipitation show greater regional variation than  
372 temperatures, with occasional conflicting trends from stations which are geographically relatively  
373 close. However, there is evidence of an increase in the quantity of precipitation with time in general  
374 except for RCP 4.5 (50%) values they are higher in 2050 than 2080 and that because of the different  
375 adapted parameters in the downscaled GCMs in that particular climate scenario. Gharbia et al.  
376 (2016b) shows that RCP 8.5 (75%) would predict the highest future precipitation quantities over the  
377 catchment. For solar radiation, all simulations indicate that there will be a significant increase in  
378 solar radiation over the Shannon catchment in the future, with such an incremental increase obvious  
379 when moving from RCP 4.5 (50%), RCP 4.5 (75%), RCP 8.5 (50%) to RCP 8.5 (75%), respectively.  
380 The relative humidity and wind speed simulation results indicate a fluctuation in values but with  
381 slight increases dominant over the Shannon catchment. Predicted increases relative humidity and  
382 wind speed are clear when moving from RCP 4.5 (50%), RCP 4.5 (75%), RCP 8.5 (50%) to RCP 8.5  
383 (75%), respectively. There are significant increases in the relative humidity and wind speed for the  
384 2050 and 2080 from the RCP4.5 (75%) and RCP8.5 (75%) projections.

385 Gharbia et al. (2016b) provides multidimensional climatological datasets and simulations for the  
386 Shannon River catchment based on four future scenarios RCP4.5(50%), RCP4.5(75%), RCP8.5(50%)  
387 and RCP8.5(75%). Thus, a significant quantity of climatological data was required to produce long-  
388 term mean monthly estimates of PETS within the Shannon River Basin District. The data source for  
389 all the baseline weather data was obtained from Met Éireann, the Irish National Meteorological  
390 Service.

391 Met Éireann is the leading provider of weather information and related services for Ireland. Observed  
392 daily data for temperature was obtained from all available stations (96 stations) in the Shannon River  
393 Basin District for the period 1961-2014. The majority of stations from which data was received can  
394 be considered low lying and of high quality. Baseline mean monthly temperature was calculated for  
395 the period 1961-2000, with the remainder reserved for calibration and evaluation processes. These  
396 data was processed within ArcGIS and a long-term mean monthly temperature raster was produced

397 for each month. As discussed previously, throughout this study the Irish National Grid coordinate  
398 system and a 50 m<sup>2</sup> cell size were employed.

### 399 Design the PETS GIS-based algorithms

400 The methodology mainly depended on the design of the PETS GIS algorithms based on the methods  
401 illustrated in the previous sections. A validation and performance evaluation process were then  
402 implemented to get the best-performing temperature-based method in order to use it in the PETS  
403 projection simulations, which were based on climate change scenarios.

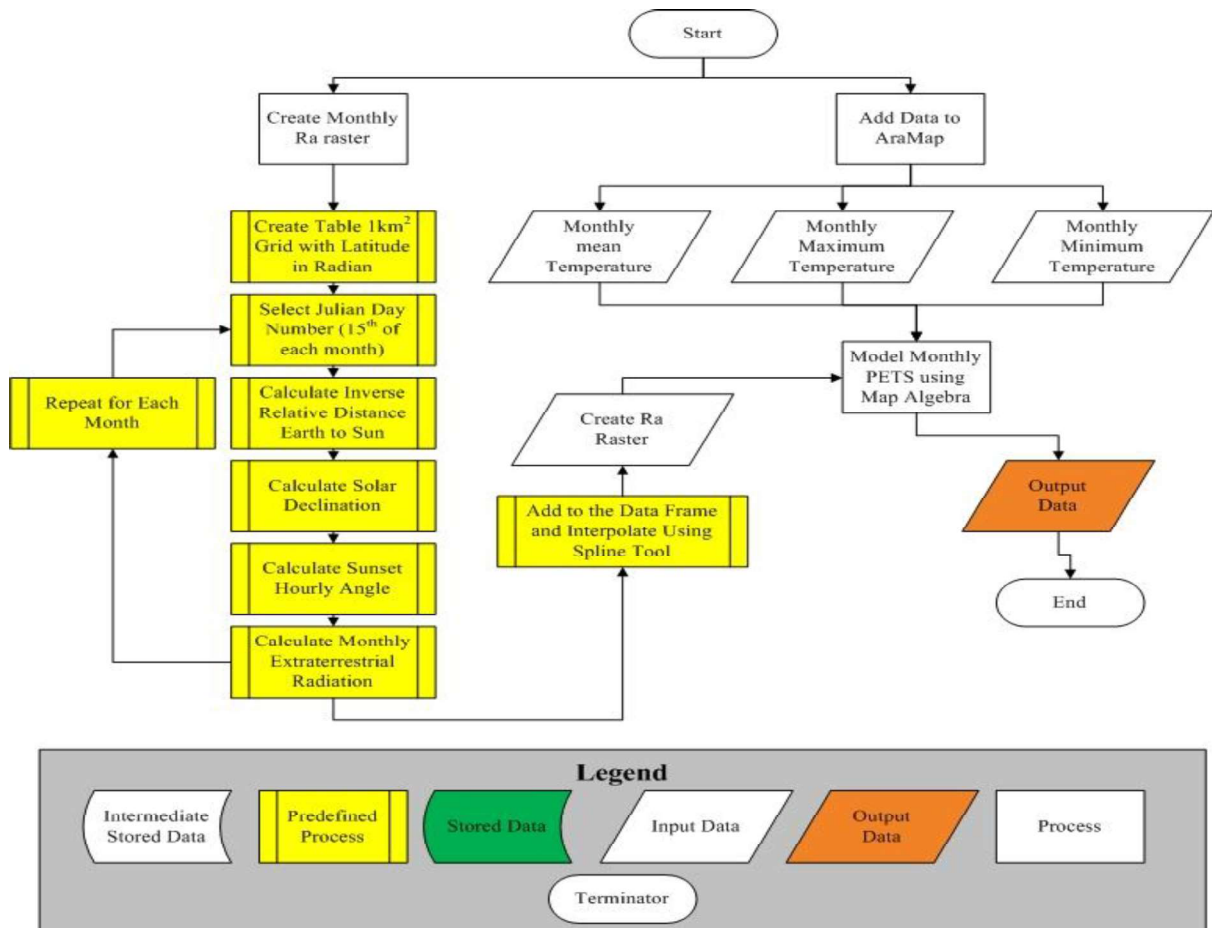
404 As discussed above, six methods were used in PETS modeling process using the designed flowcharts  
405 below, in some of these flowcharts the interpolation is used. As all the used methods are temperature  
406 based methods, and temperature as an atmospherically parameters is relatively smoothly spatially  
407 distributed parameter, and as the Shannon River catchment is relatively flat catchment without any  
408 really high mountains, so the Spline spatially interpolation method is used in all the methods.

409

#### 410 • **Hargreaves and Samani**

411 The Hargreaves and Samani method was one of the most complex methods applied during this study.  
412 A flow chart of the methodology used in modeling PETS using this method is shown in Figure 2,  
413 based on the spatially distributed calculation process for the previously discussed equations.

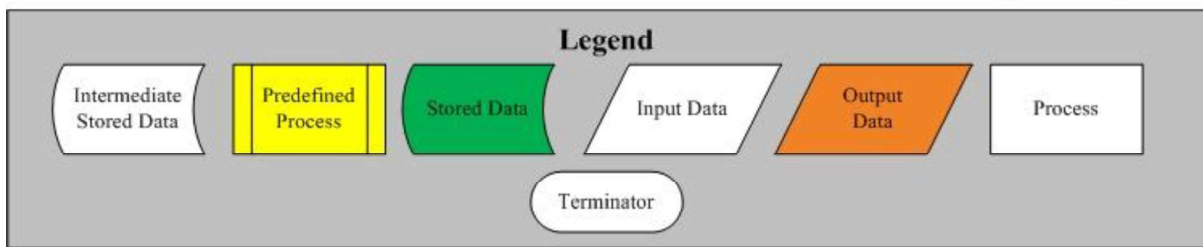
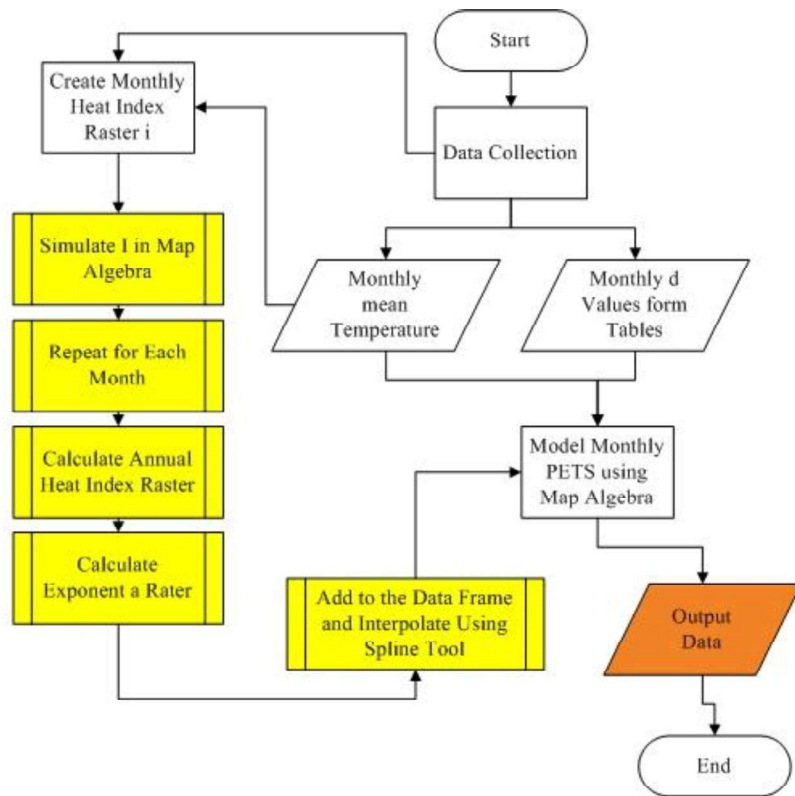
414



415  
416 **Figure 2: Hargreaves and Samani designed algorithm flowchart.**

417 • **Thornthwaite**

418 The Thornthwaite method was completed using a similar methodology to the Hargreaves and Samani  
 419 method using the designed algorithm flowchart illustrated in Figure 3. Monthly heat index values  $I$ ,  
 420 previously illustrated, were estimated from mean monthly temperatures. A raster file of  $i$  was  
 421 created for each month, and then summed to produce a raster file of  $I$ . Once  $I$  had been calculated it  
 422 was possible to create a raster of exponent  $a$ , then produce the PETS monthly raster maps.



423

424

**Figure 3: Thornthwaite designed algorithm flowchart.**

425

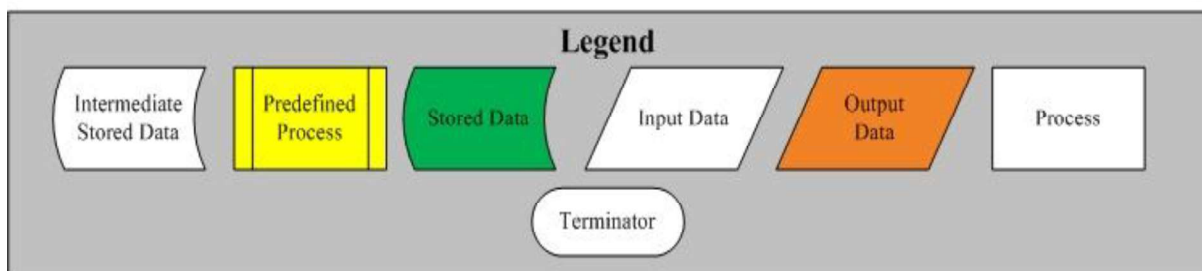
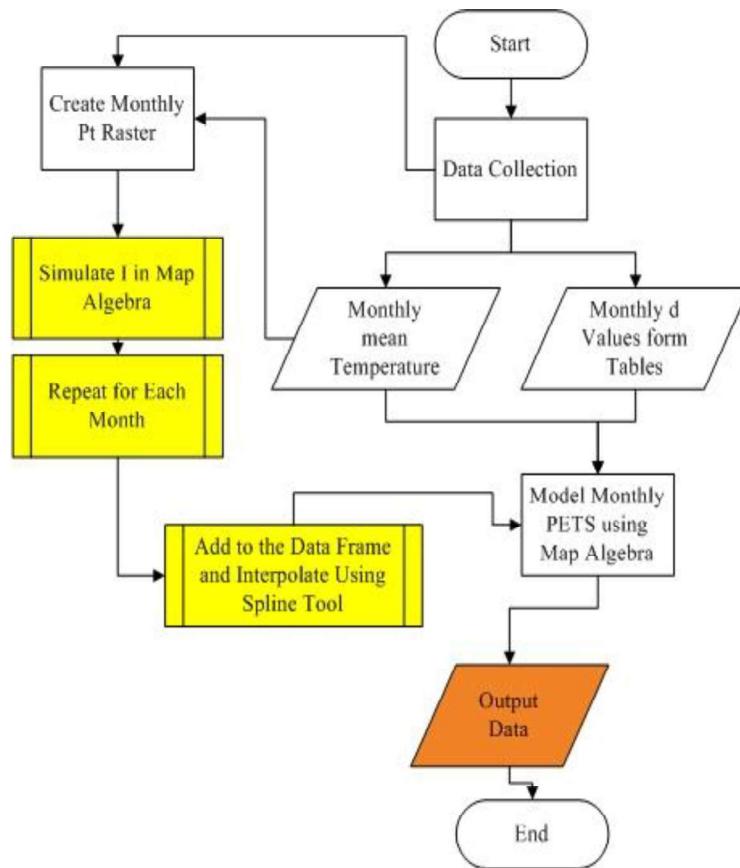
- **Hamon**

426

Similar to the preceding methods, the Hamon method required pre-processing to create monthly

427

raster files of variable Pt. The designed algorithm flowchart for this method illustrated in Figure 4.



428

429

**Figure 4: Hamon designed algorithm flowchart.**

430

- **Blaney-Criddle and Kharrufa**

431

The Blaney-Criddle and Kharrufa methods were among the simplest methods applied within this

432

study. Their application required mean monthly temperature rasters and monthly values for p, once

433

retrieved the methods could be readily applied within the ArcMap GIS environment. The designed

434

algorithm flowchart for this method illustrated in Figure 5. The represented flow chart in the Figure 5

435

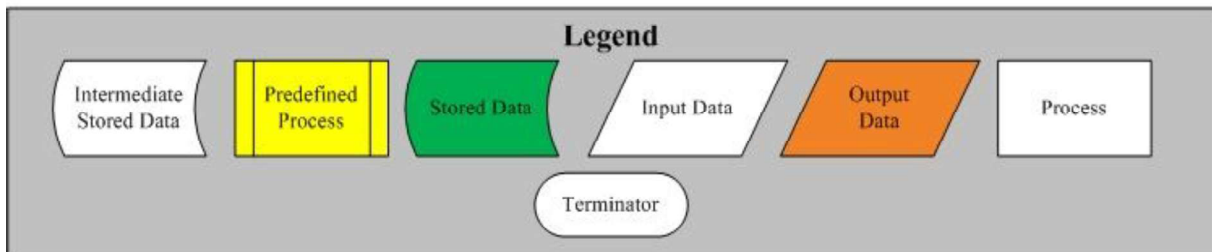
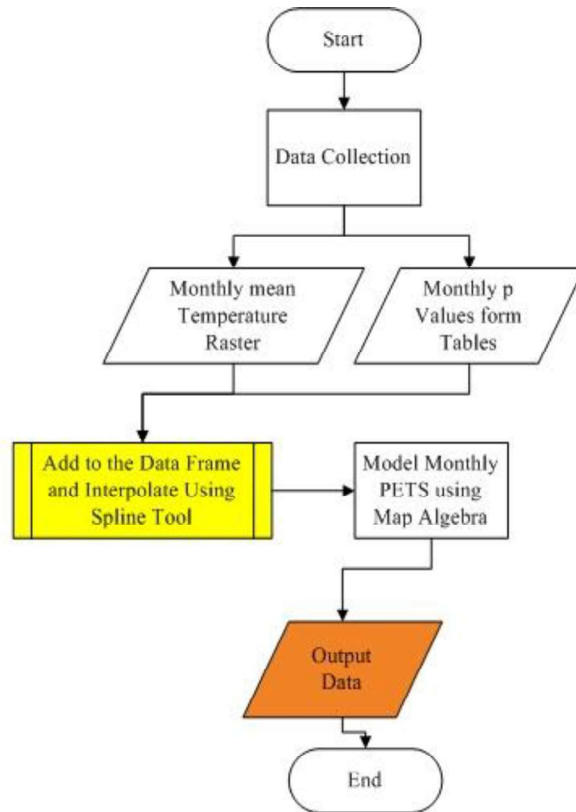
represents a practical simplification to the Eq 1, as the two input parameters in the equation are

436

prepared in the raster data format then they used in the map algebra processor in the ArcMap to make

437 the PETS calculation according to the Eq 1.

438



439

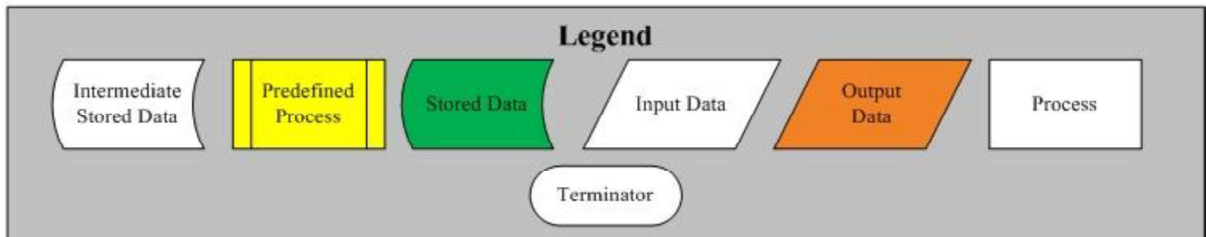
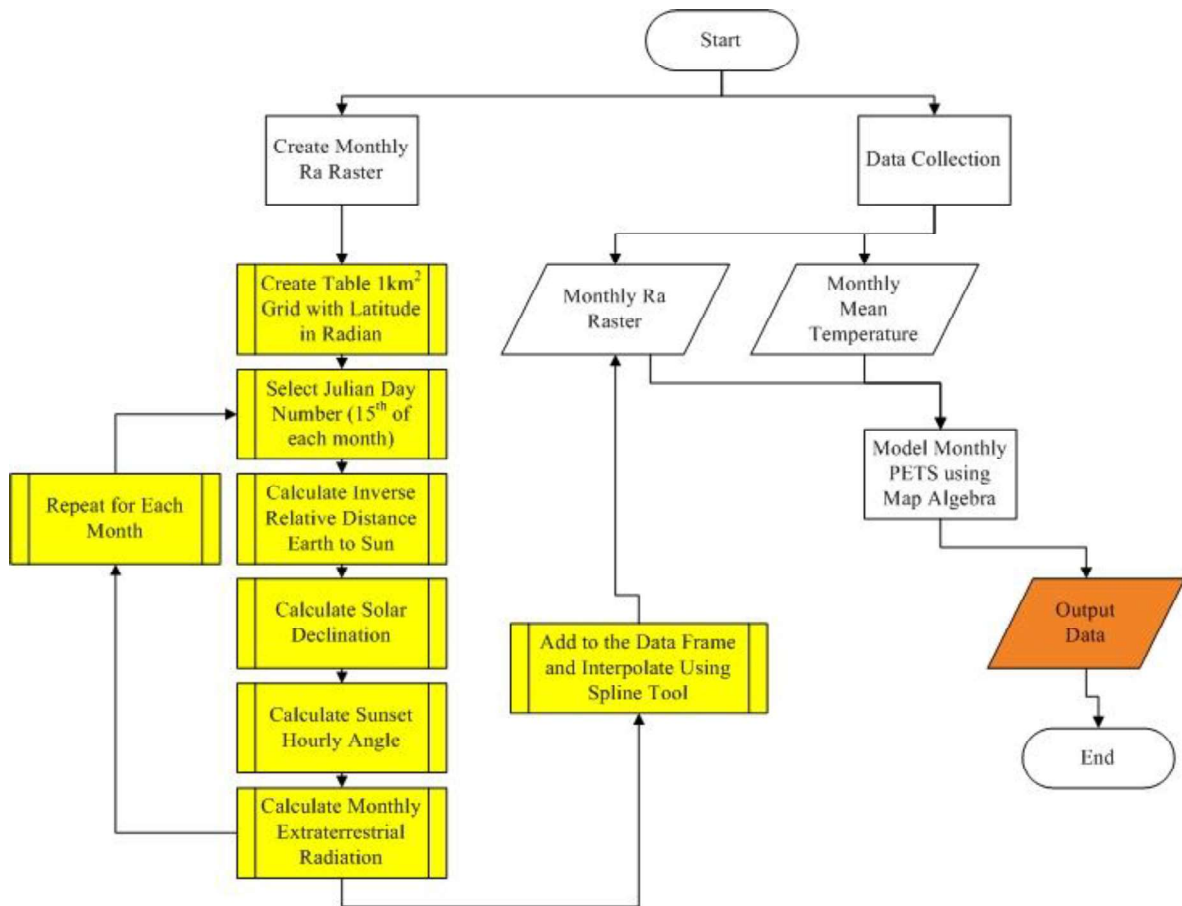
440

**Figure 5: Blaney-Criddle and Kharrufa designed algorithm flowchart.**

441

442 • **Oudin**

443 The Oudin method was similar in its application to the Hargreaves and Samani method described  
444 previously, requiring mean monthly temperature data and estimates of monthly extraterrestrial  
445 radiation as shown in Figure 6.



446

447

**Figure 6: Oudin designed algorithm flowchart.**

448 Validation and performance evaluation

449 Short-term (2012-2015) mean monthly PETS rates for four synoptic weather stations within the  
 450 Shannon River Basin District were obtained from Met Éireann. The four synoptic stations are listed  
 451 in Table 2 with their respective elevation and the percentage of the valid data, their locations are  
 452 shown in Figure 1. The resultant baseline mean monthly PETS values at the same location as the  
 453 synoptic meteorological stations from each of the six selected models were compared with that of the  
 454 short-term mean monthly PETS data from the Met Éireann stations (which are calculated by Penman-

455 Monteith method). The evaluation of the performance of the PETS models was completed on both  
 456 a graphical and statistical basis. The modeled values were evaluated based on a number of  
 457 statistical values. Firstly, the coefficient of determination ( $R^2$ ) was determined for each data set,  
 458 which is a statistical measure of how close the data are fitted to the trusted data. Similarly, the root  
 459 means square error (RMSE), which is a measure of the difference between modeled values and the  
 460 trusted values was calculated. The mean absolute percentage error (MAPE), which is a measure  
 461 of prediction error, in %, of the model was also calculated. Finally, the mean absolute deviation  
 462 (MAD) was calculated, which measures the size of the error between the two sets of data.

463

464 **Table 2: Synoptic meteorological stations within the Shannon River Basin District.**

Location	Elevation (meter above mean sea level)	Percentage of valid data (%)
Mullingar	101	88
Mount Dillon	39	84
Gurteen College	75	87
Shannon Airport	6	97

465

#### 466 [Climate change effects on PETS](#)

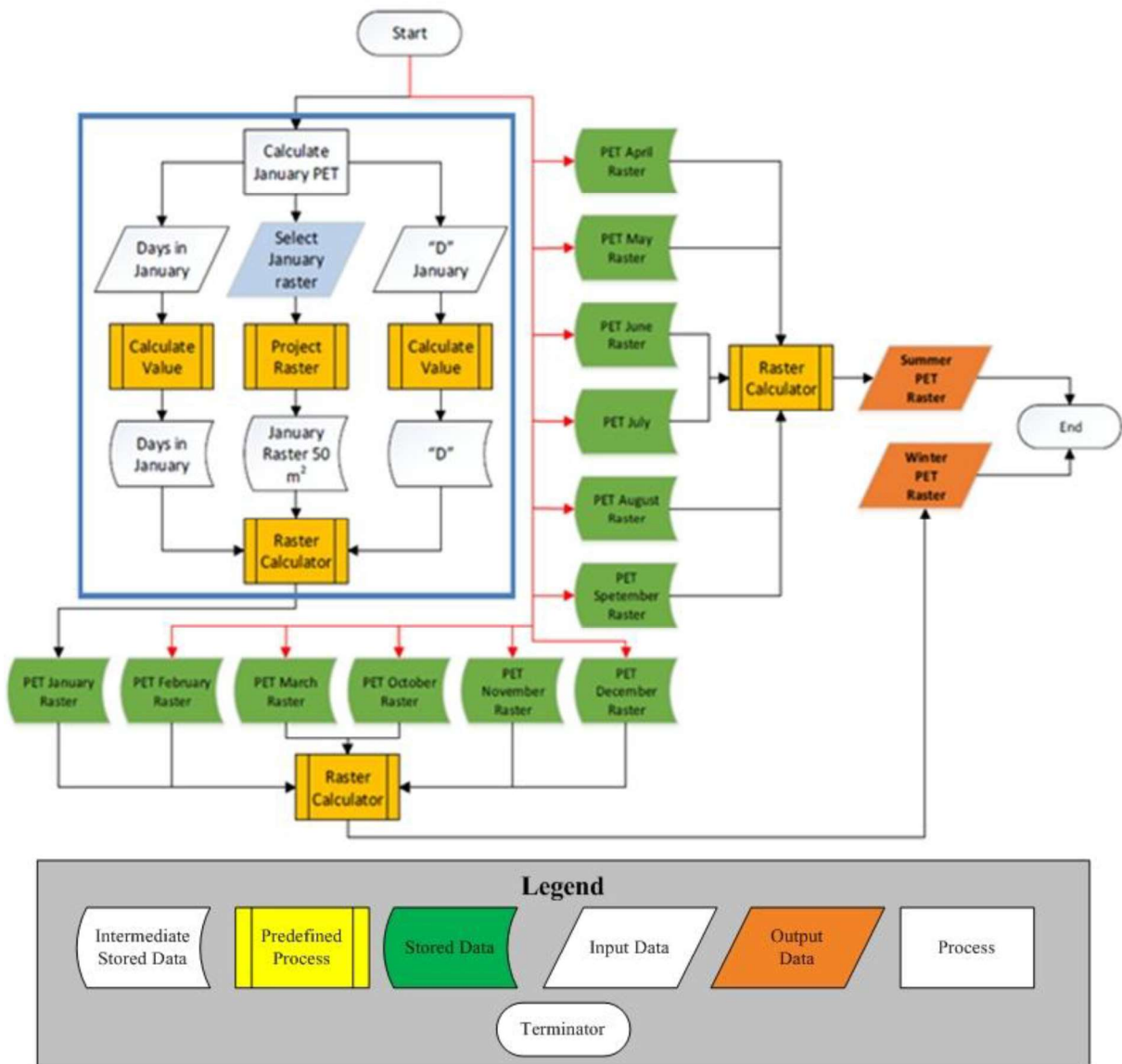
467 Upon assessment, it was found that the results from the Hamon method best correlated with the  
 468 data available from the synoptic stations. In that regard, the Hamon method was selected for modeling  
 469 changes in future PETS within the Shannon River Basin District as a consequence of climate change.

470

471 Climate change projections for the Shannon River Basin District were obtained for several climate  
 472 variables from Gharbia et al. (2016b), including mean monthly temperature, from multi-GCM  
 473 ensembles for three future time intervals (2020, 2050 and 2080) using a range of different  
 474 Representative Concentration Pathways (RCPs). The climate change models were based upon two  
 475 different RCPs; using a radiative forcing of 4.5 W/m<sup>2</sup> and 8.5 W/m<sup>2</sup> respectively, which were  
 476 produced from 50% (median) and 75% (3rd quartile) multi-GCM ensembles simulation results.

477

478 The Hamon method was applied to three future time intervals each including four possible climate  
479 scenarios, each requiring PETS to be estimated for twelve months; thus, it was required for the  
480 Hamon method to be applied for 144 monthly scenarios. A methodology flowchart for the algorithm  
481 created under the GIS environment is shown in Figure 7; where all processes encompassed in blue are  
482 applicable prior to all output rasters shown in green, simply Figure 7 can be described as a loop for  
483 the Figure 4 in order to get all the maps according to all the climate scenarios in monthly time step.



484

485

**Figure 7: PETS projection designed algorithm flowchart.**

486

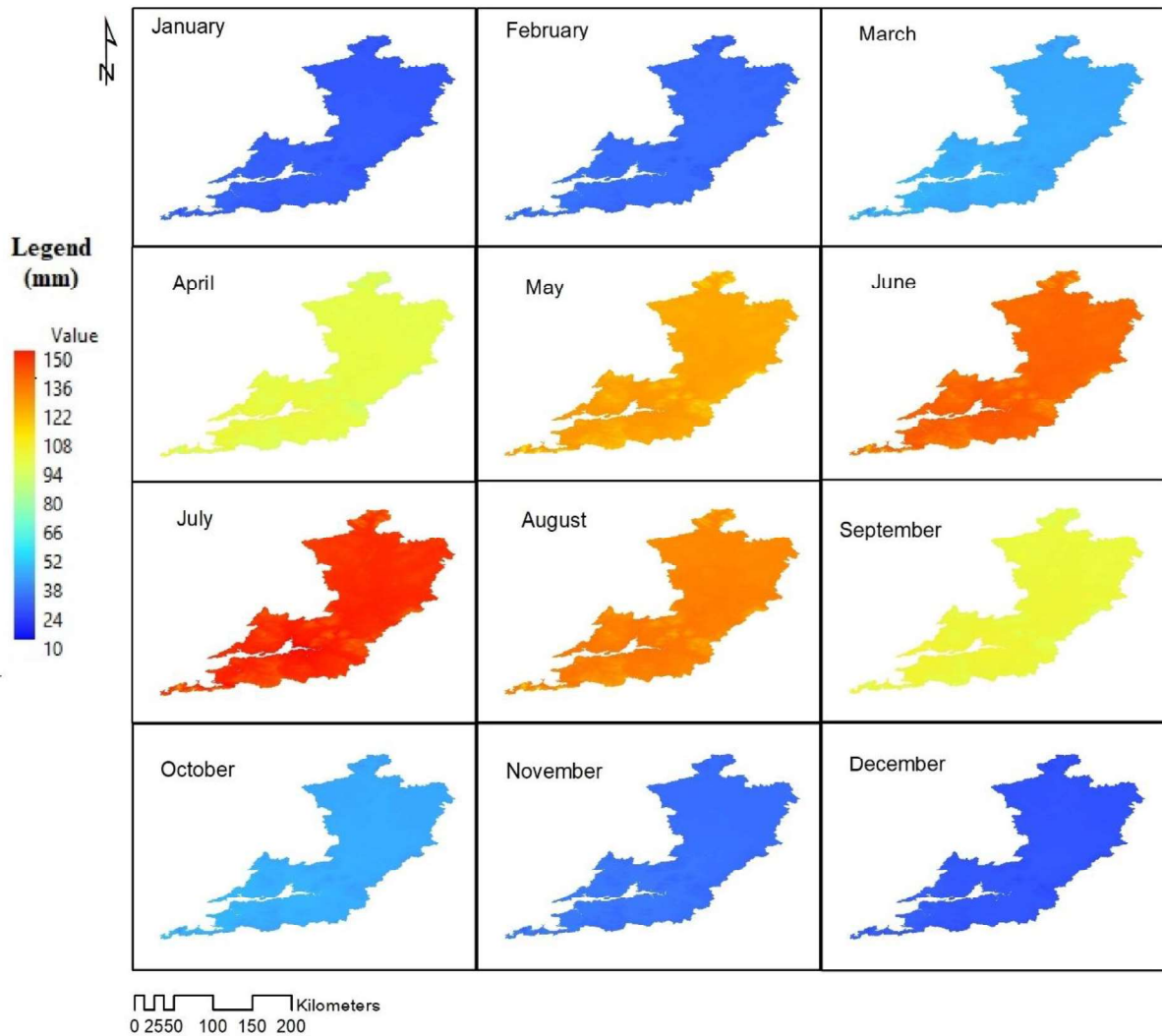
## *Results and Discussions*

### 487 Baseline PETS monthly simulation

488 The 6-selected empirical temperature based PETS formulae were applied to long-term mean monthly  
489 temperature data for the Shannon River Basin District within a GIS. For each approach, a raster map  
490 of the Shannon River Basin District was created for each month of the year. These rasters depict the  
491 long-term mean monthly PETS throughout the region in mm. The raster maps created are presented  
492 below.

#### 493 • **Blaney-Criddle**

494 The Blaney-Criddle method estimates PETS based on mean monthly temperature and sunshine hours;  
495 rasters created using this approach are shown in Figure 8. Figure 8 shows that in general a significant  
496 increase in the PETS occurs in July. The simulated spatially distributed pattern of PETS using  
497 Blaney-Criddle has a significant change over the different maps shown in Figure 8.



498

499

**Figure 8: Blaney-Criddle baseline monthly PETS raster maps.**

500

- **Kharrufa**

501

Similarly, to the Blaney-Criddle approach, the Kharrufa method uses mean monthly temperature and

502

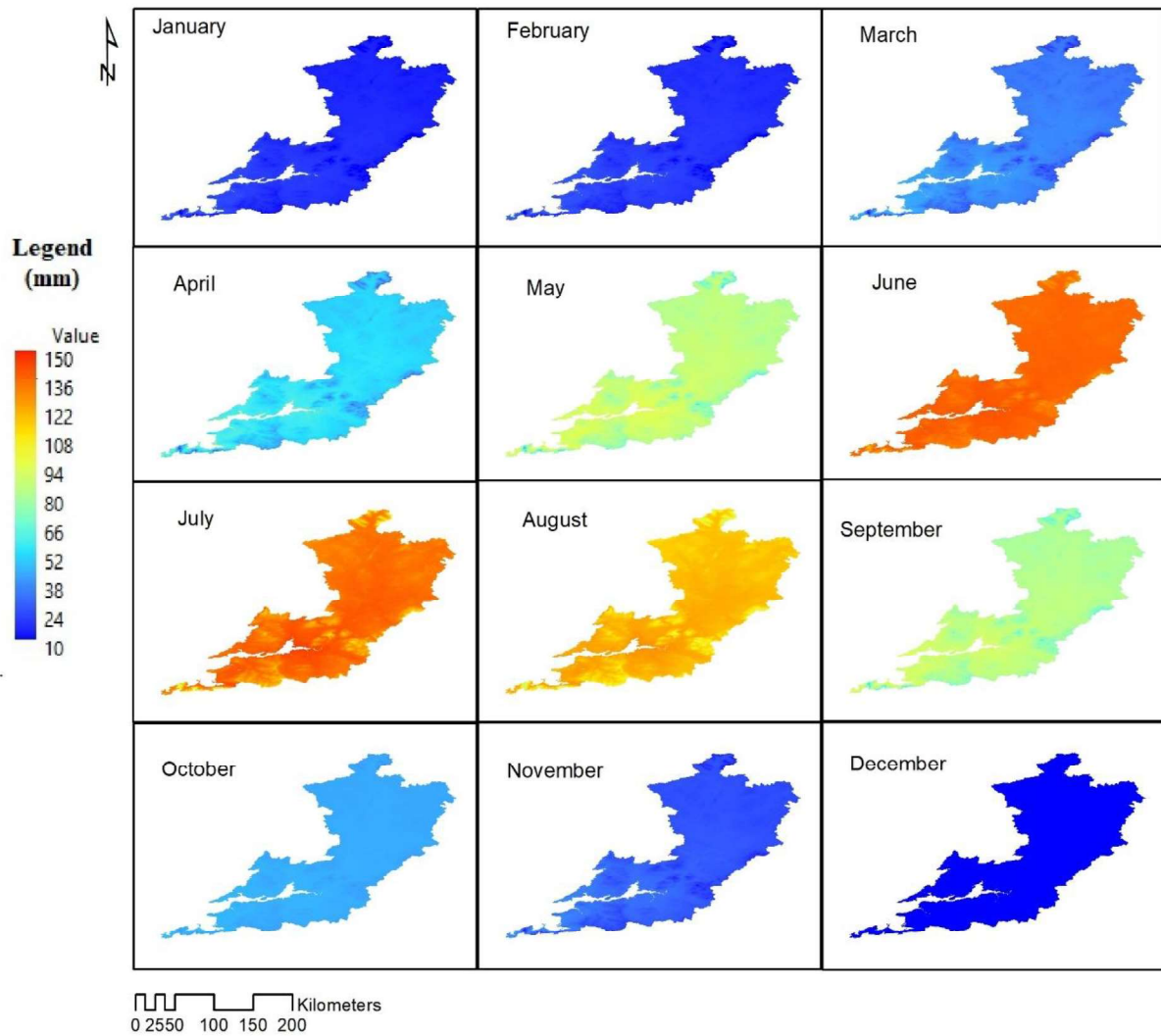
sunshine hours to estimate PETS; raster maps created by means of this approach are presented in

503

Figure 9. Figure 9 shows that Karrufa method produces almost the same spatially distributed patterns

504

of PETS using Blaney-Criddle over all the simulated months.



505

506

**Figure 9: Kharrufa baseline monthly PETS raster maps.**

507

- **Hargreaves and Samani**

508

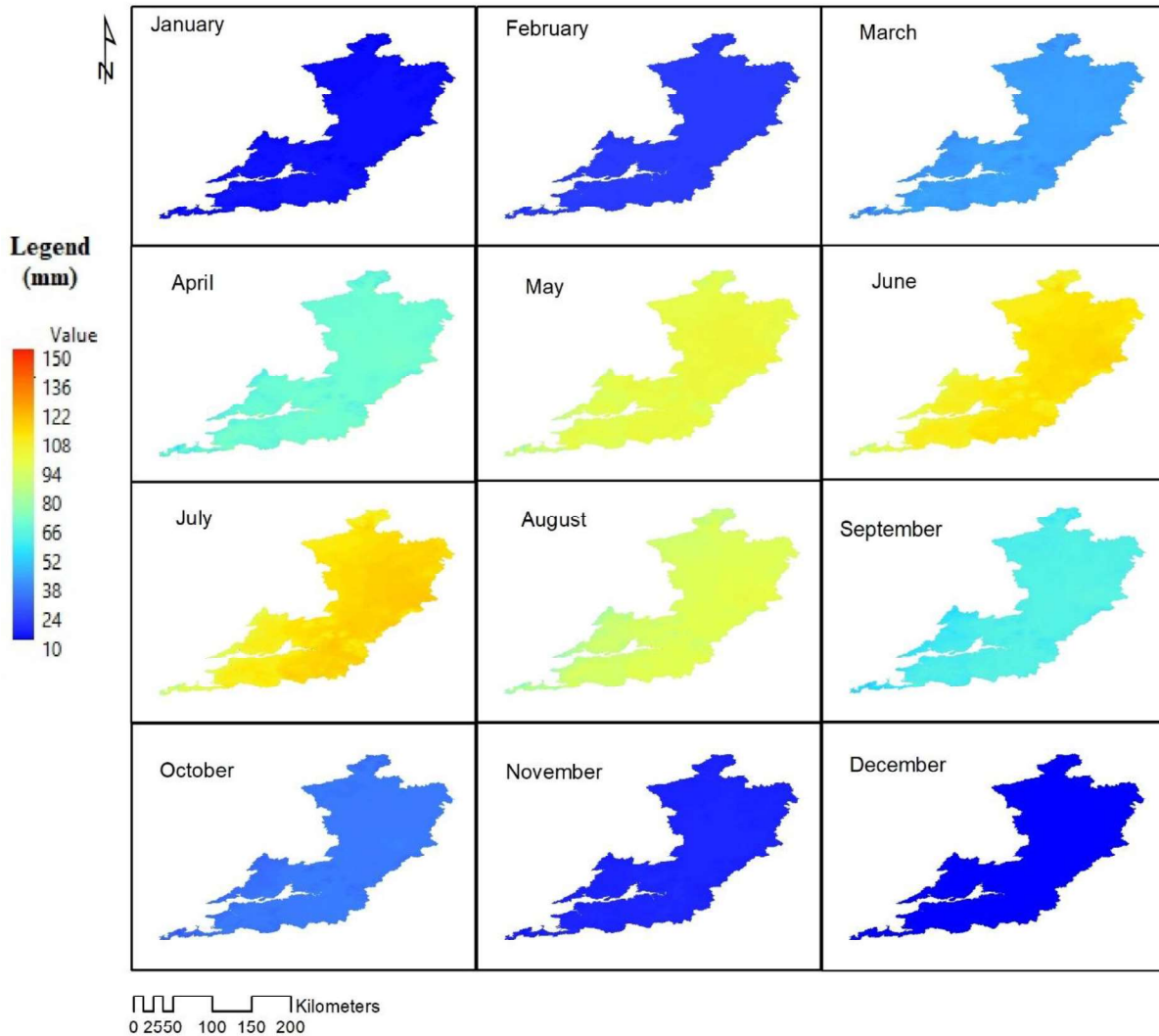
This approach represents one of the most complex applied during this study, requiring a minimum, maximum and mean temperature data as well as extra-terrestrial radiation. Raster map created using this approach are presented in Figure 10.

511

Figure 10 shows that Hargreaves and Samani method has almost the same spatially distributed patterns shown on all the simulated PETS maps except for December, January and February, their spatially distributed patterns have significant differences from others. Hargreaves and Samani method provides good spatially distributed estimations for the PETS. In general, this method fails to estimate

514

515 the hot spot areas in terms of both the locations and the values. Hargreaves and Samani provides over  
516 estimated values in most of the eastern parts of the catchment and less estimated PETS values for the  
517 western part of the catchment.



518

519

**Figure 10: Hargreaves and Samani baseline monthly PETS raster maps.**

520

- **Oudin**

521

522

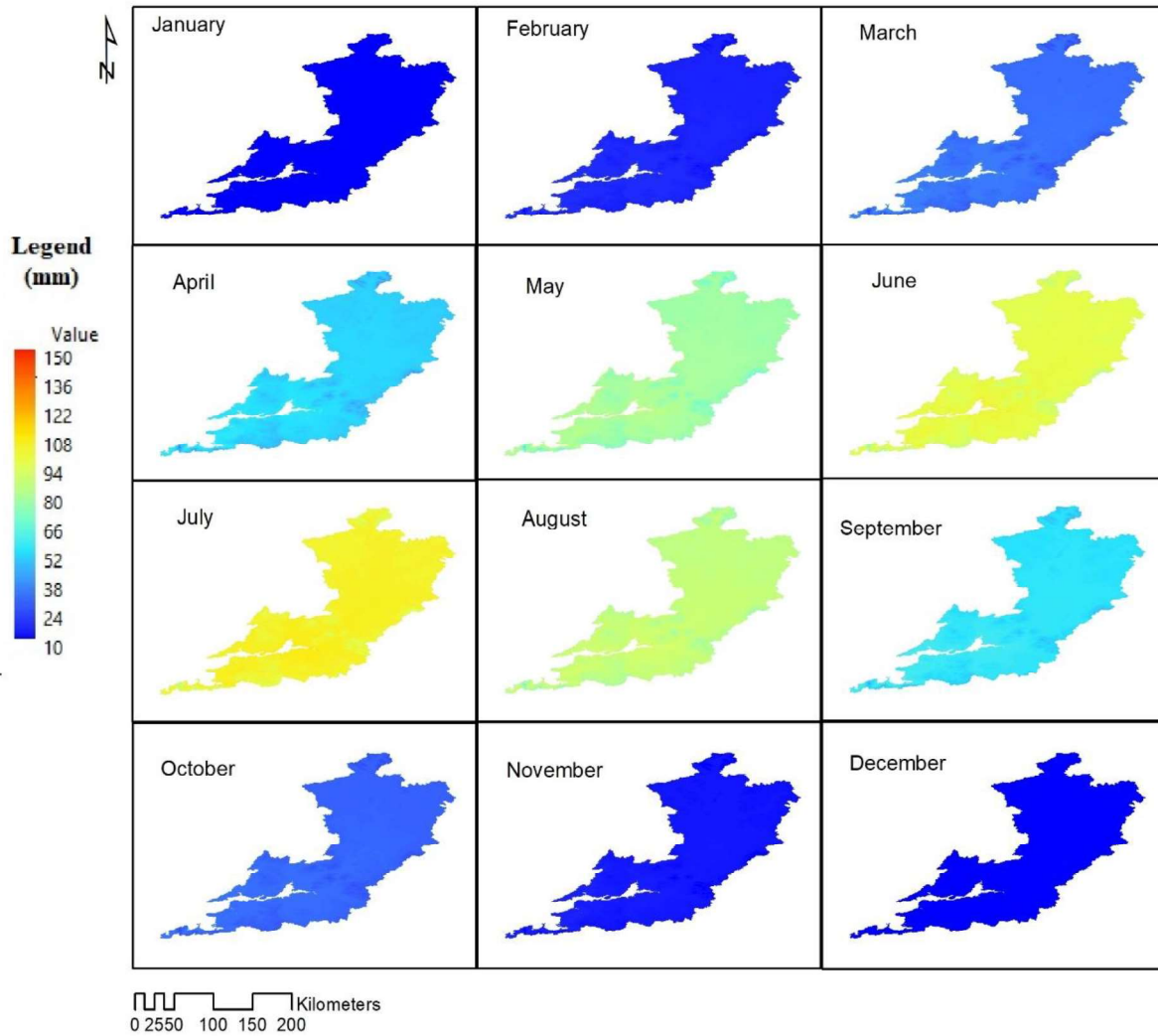
523

524

The equation presented by Oudin also requires extra-terrestrial radiation data, however unlike the Hargreaves and Samani only mean monthly temperature is required. Raster maps prepared using this method are shown in Figure 11. Oudin method provides very good spatially distributed estimations for the PETS. In general, this method provides good estimates for the hot spot areas in terms of both

525 the locations and the values. Oudin provides over estimated values in the southern part of the  
526 catchment, which is mainly due to the location on the coastal areas.

527



528

529

**Figure 11: Oudin baseline monthly PETS raster maps.**

530

- **Thornthwaite**

531

The Thornthwaite method uses mean monthly temperature to estimate both a radiation term and

532

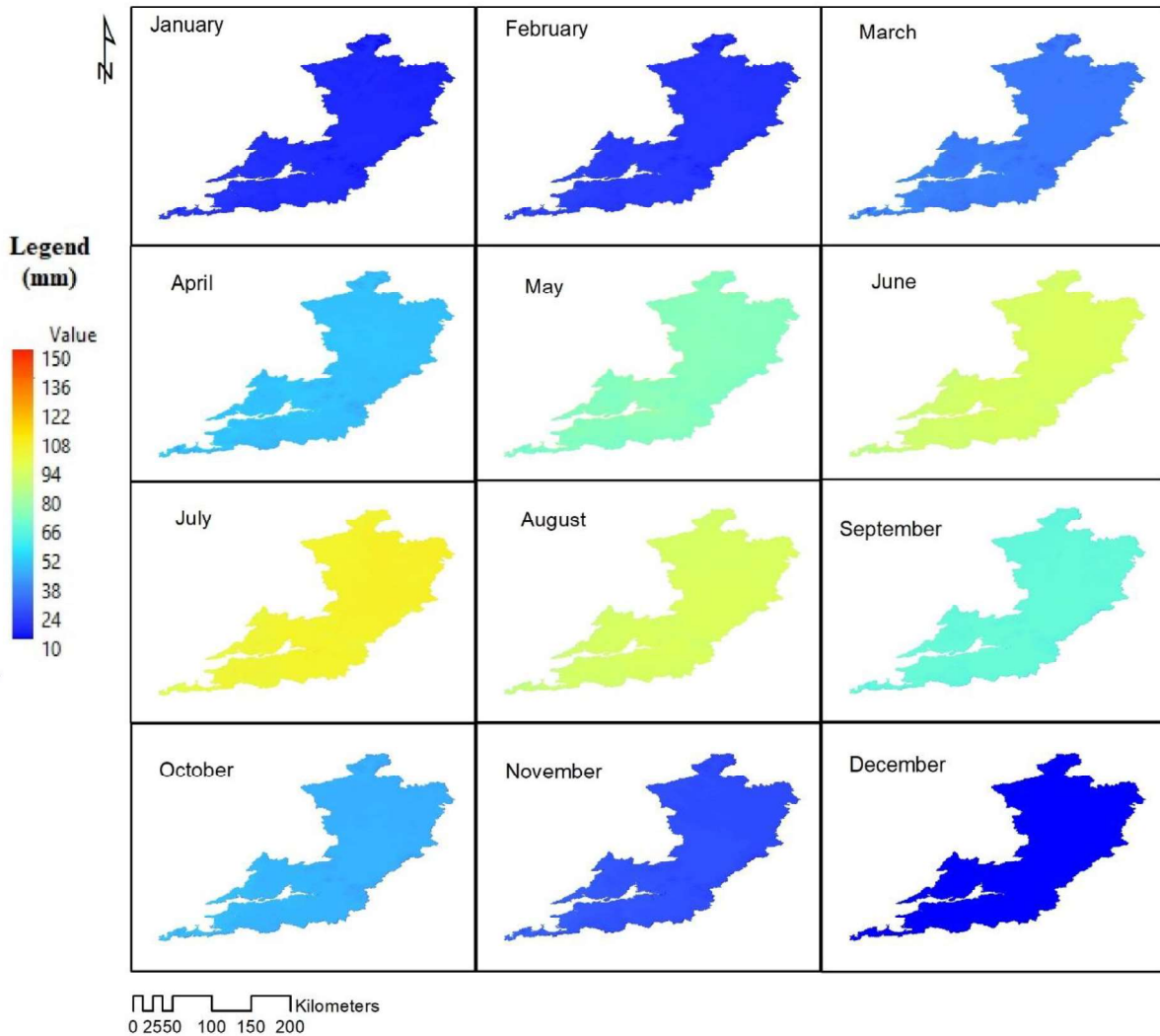
PETS; raster maps are presented in Figure 12. Thornthwaite method has the lowest simulated PETS

533

values for September, October and November with unique spatially distributed patterns for all of them

534

compared with the other used methods, see Figure 12.



535

536

**Figure 12: Thornthwaite baseline monthly PETS raster maps.**

537

- **Hamon**

538

PETS is estimated based on mean temperature, which is used to calculate a vapor density term, and

539

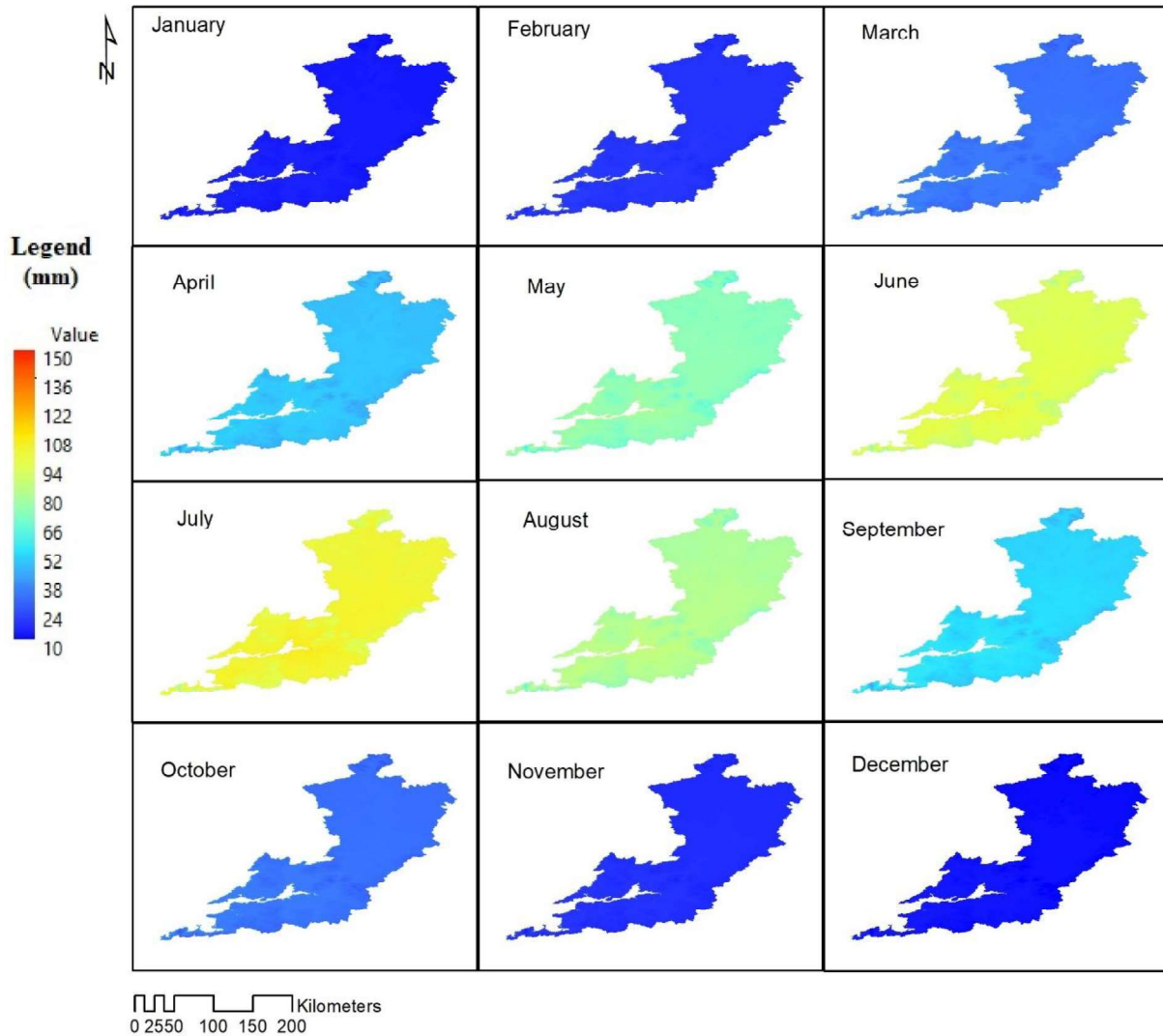
daylight hours; raster maps created are presented in Figure 13. Hamon method appears to be the most

540

consistent method to simulate the PETS between summer and winter. This method has almost one

541

spatially distributed PETS pattern for summer months and another different one for winter months.



542

543

**Figure 13: Hamon baseline monthly PETS raster maps.**

544

Each empirical method applied successfully produced a spatially distributed estimation of long-term

545

mean monthly PETS for the Shannon River Basin District. From initial inspection of the results, each

546

method appears to produce reasonable estimates of PETS throughout the region; with minimal PETS

547

rates during cold winter months and higher rates (up to 100+ mm per month) during summer months.

548

In addition, a clear variation in PETS is visible in coastal areas in the southwest of the region which

549

would be expected. However, from inspecting the raster maps produced it was not possible to

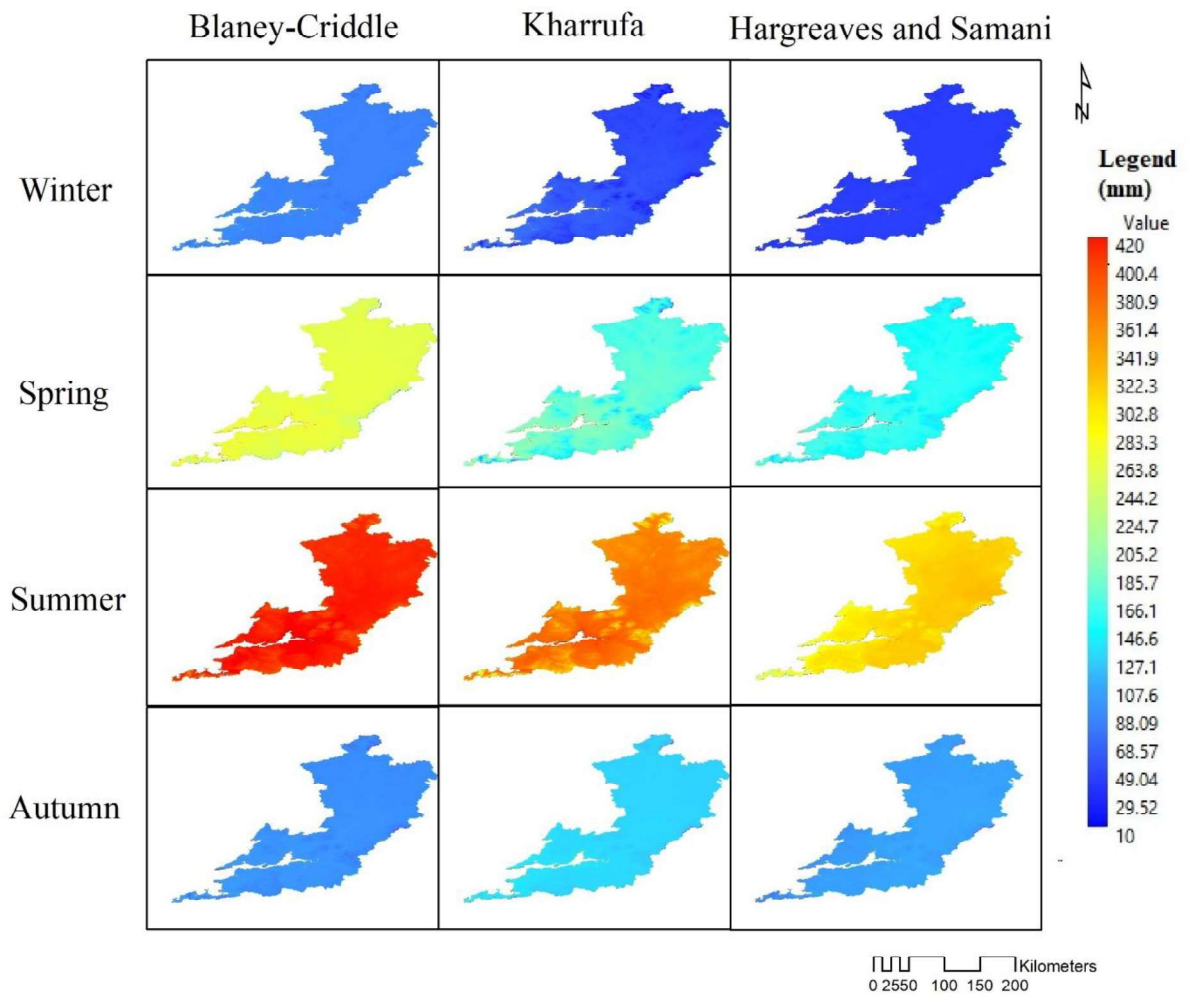
550

determine the most accurate method for use within the Shannon River Basin District. Thus, further

551

evaluation of the methods was necessary and is discussed in the following section. Figures 141-15

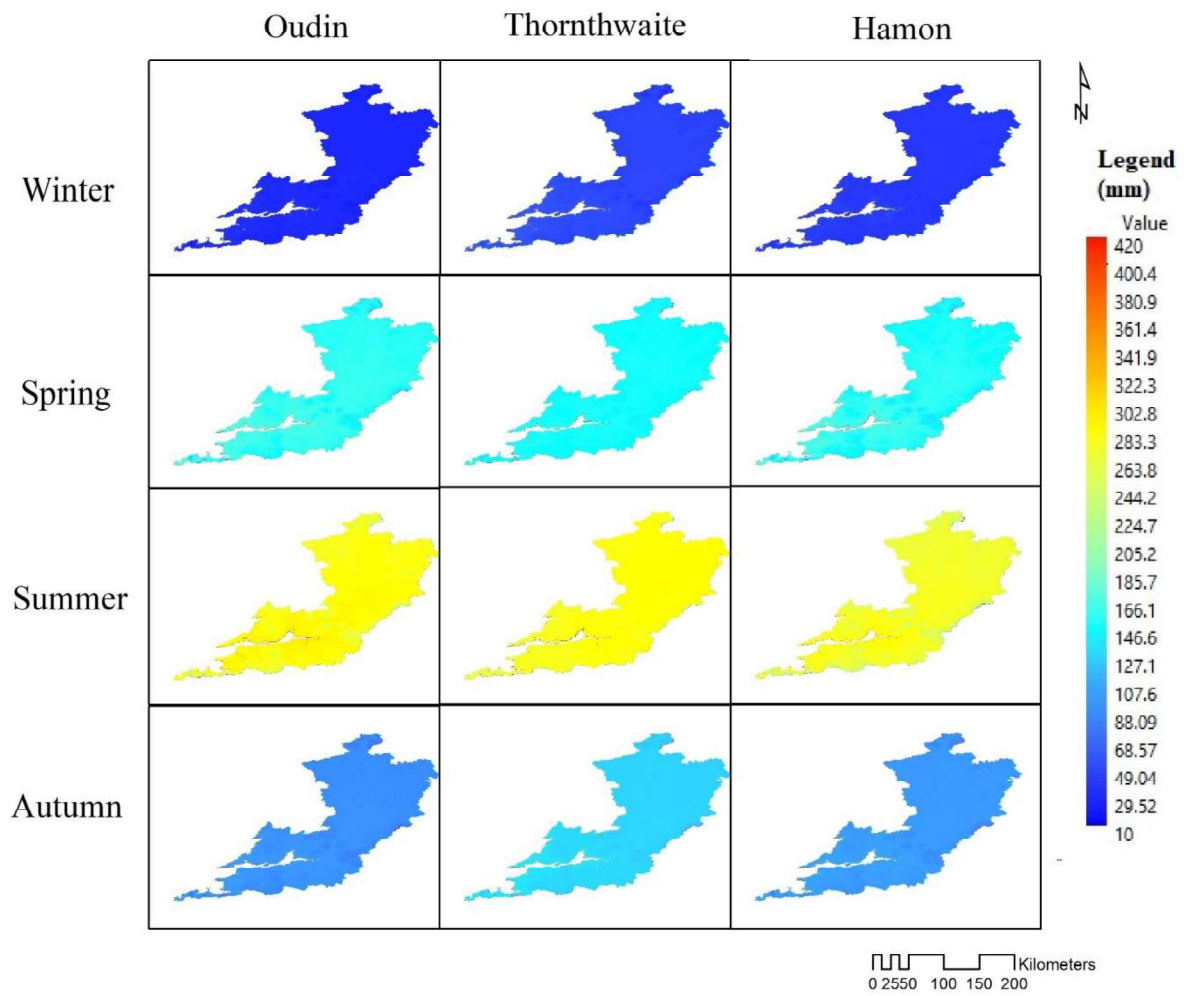
552 show the seasonally comparison between the simulation methods for the baseline period.



553

554 **Figure 14: comparisons between the seasonally simulated baseline PETS raster maps (Blaney-**

555 **Criddle, Kharrufa and Hargreaves and Samani).**



556

557 **Figure 15: comparisons between the seasonally simulated baseline PETS raster maps (Oudin,**

558 **Thornthwaite and Hamon).**

559

## 560 Validation and performance evaluation

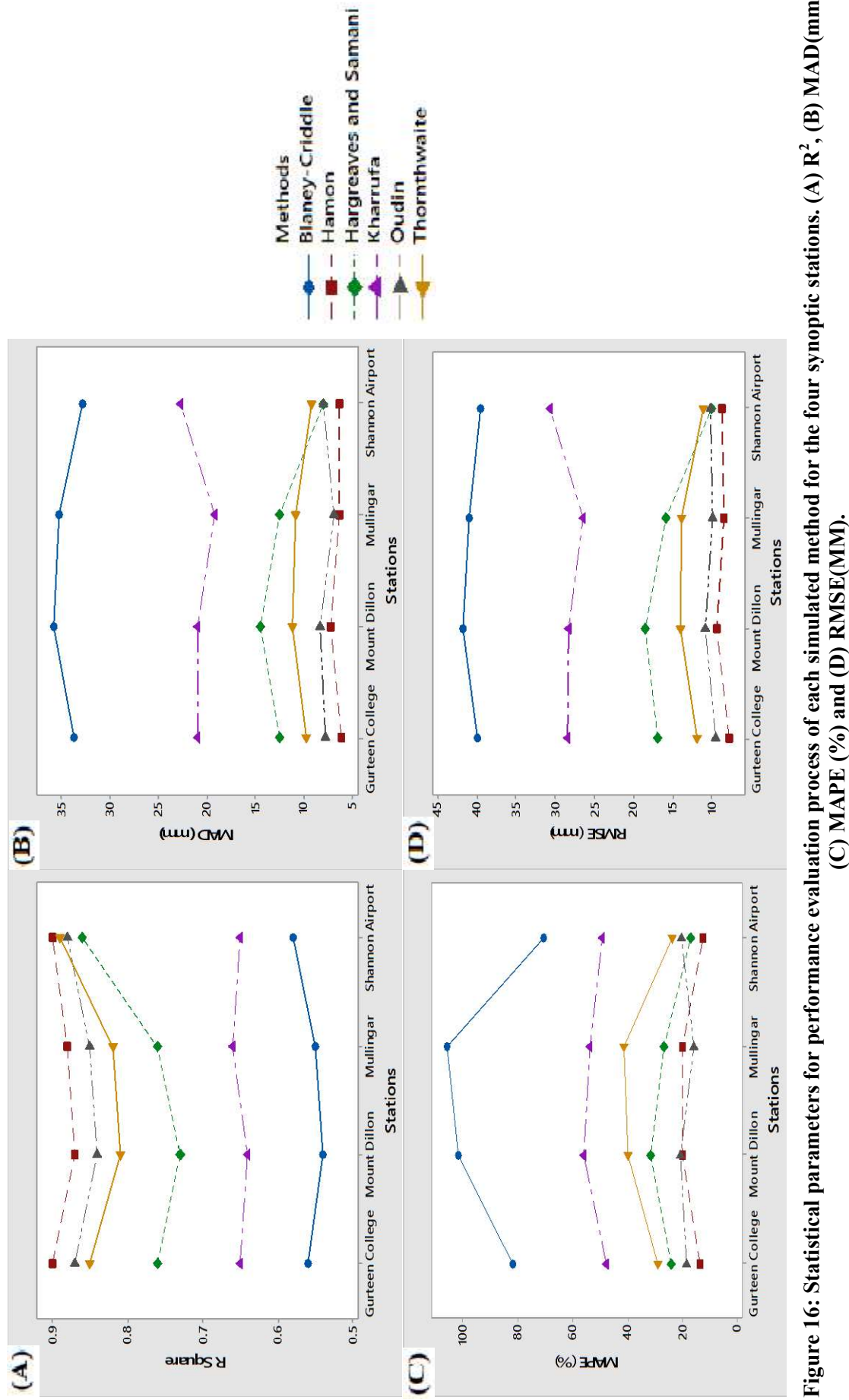
561 The modeled values in this study were evaluated against the secured Penman-Monteith PETS values  
562 of the four Met Éireann synoptic stations, based on a number of statistical values, which are  $R^2$ ,  
563 RMSE, MAPE and MAD. These statistical values were calculated for each of the four locations and a  
564 mean value was taken for each, which shown in Figure 16. Evaluation of Blaney-Criddle modeled  
565 PETS values is presented in Figure 16 below. From the results, there is a clear disparity between the  
566 datasets at all four locations. This is further demonstrated by the low  $R^2$  and high RMSE, MAPE and  
567 MAD values.

568 Similarly, results from the Kharrufa method are evaluated in Figure 16 below. Although a more  
569 simplified approach the Kharrufa method returned somewhat more accurate results with a mean  $R^2 =$   
570  $0.652$ , RMSE = 28.5 mm, MAPE = 51.5% and MAD = 20.9 mm.

571 Given the relative complexity of the Hargreaves and Samani method, one would have the expectation  
572 that the method would return somewhat accurate results. As it can be seen from Figure 16 the  
573 modeled results are significantly more accurate the previous methods with a mean  $R^2 = 0.774$ , RMSE  
574 = 15.3 mm, MAPE = 24.8% and MAD = 11.8 mm.

575 Similarly to the Hargreaves and Samani method, the Oudin method also produced  
576 significantly improved estimates compared to the preceding methods as shown in Figure 16, with a  
577 mean  $R^2 = 0.860$ , RMSE = 10.1 mm, MAPE = 18.6% and MAD = 7.7 mm. Similarly, given the  
578 relative complexity of the Thornthwaite method, one would have the expectation of more accurate  
579 estimates of PETS compared to some of the most simple methods. As it can be seen from Figure 16 it  
580 did return relatively accurate results with a mean  $R^2 = 0.841$ , RMSE = 12.7 mm, MAPE = 33.3% and  
581 MAD = 9.2 mm. Finally, results of the Hamon method are presented in Figure 16. The fact that the  
582 Hamon method may be considered one of the more simple methods applied as part of this study it  
583 returned the best mean  $R^2 = 0.888$ , RMSE = 8.6 mm, MAPE = 16.5% and MAD = 6.5 mm. In order  
584 to more clearly delineate the deviance between modeled and Met Éireann values, monthly PETS  
585 values were plotted for each location and are provided in Figure 17. From the figure, it is evident that,  
586 particularly during summer months (April-September), the PETS models consistently overestimate

587 PETS. That might be because all the methods are not calibrated against the Irish summer long daytime  
588 and calibrating them was not possible due to the lack of observed evapotranspiration data. This  
589 overestimation is not really significant, so the validated methods can still be used in the Irish  
590 environment. During winter months (October-March) modeled results correspond more closely with  
591 the Met Éireann values, although it must also be considered that during this period PETS rates are at  
592 their lowest. Through the evaluation of the statistical results presented in Figure 16 and examination  
593 of Figure 17 the Hamon method was selected as the most appropriate method for application within  
594 the Shannon River Basin District and thus was selected for application in the final stage of this  
595 study, the results of which are presented within the following section. It could be concluded that  
596 Hamon method was performing the best for the Shannon catchment because of the simple  
597 parameterization which includes two main factors, the daytime period and the temperature, with an  
598 exponential relation which is one of the main difference between Hamon and the other methods.



599

600

601

Figure 16: Statistical parameters for performance evaluation process of each simulated method for the four synoptic stations. (A) R<sup>2</sup>, (B) MAD(mm), (C) MAPE (%) and (D) RMSE(MM).

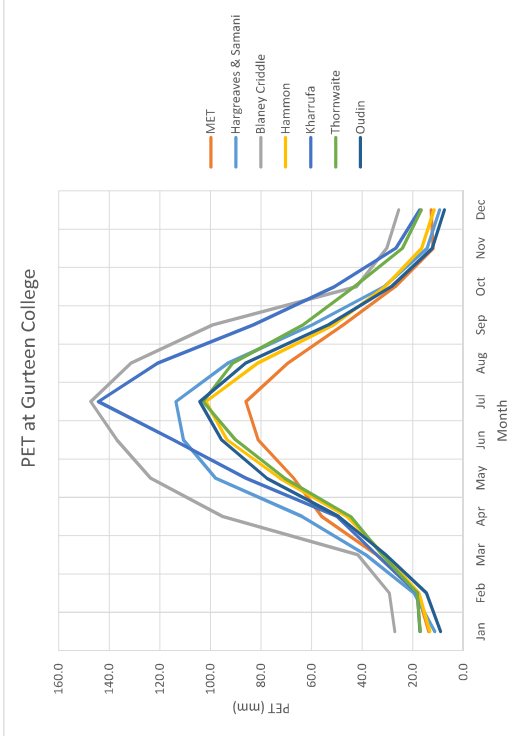
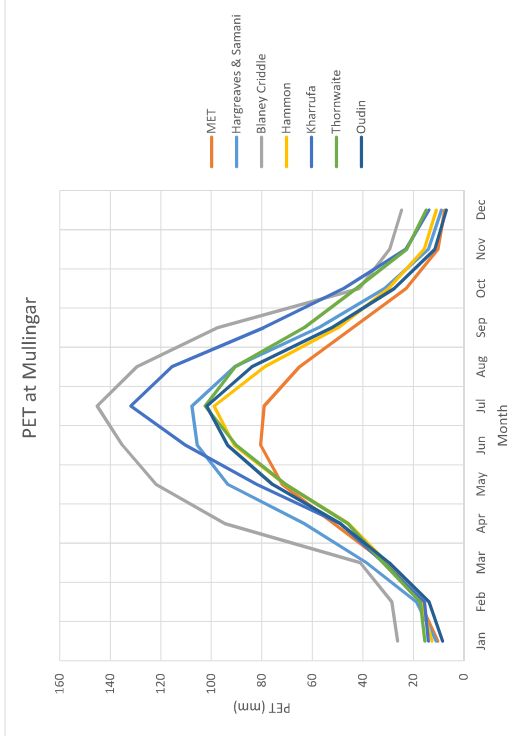
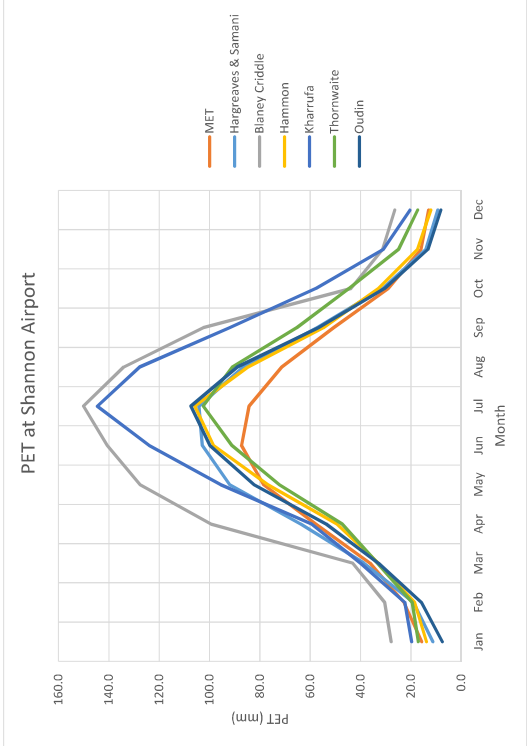
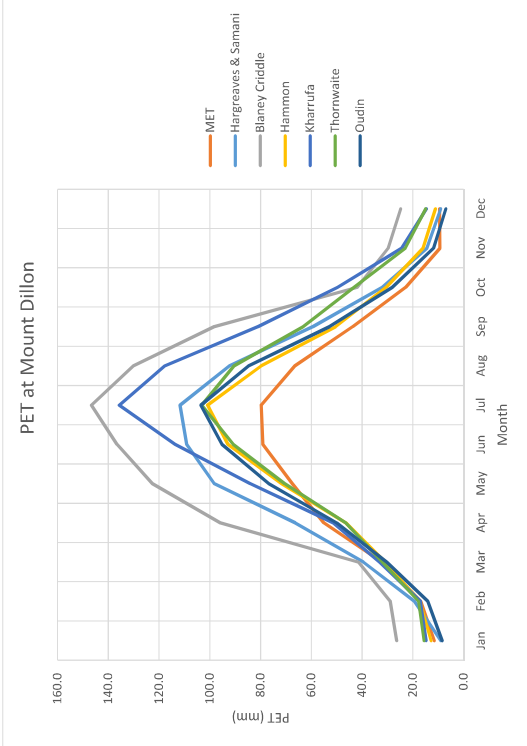


**Figure 17: Met Éireann and modeled monthly PETs at four synoptic stations located in the Shannon River Basin District.**

604 Future PETS simulations

605

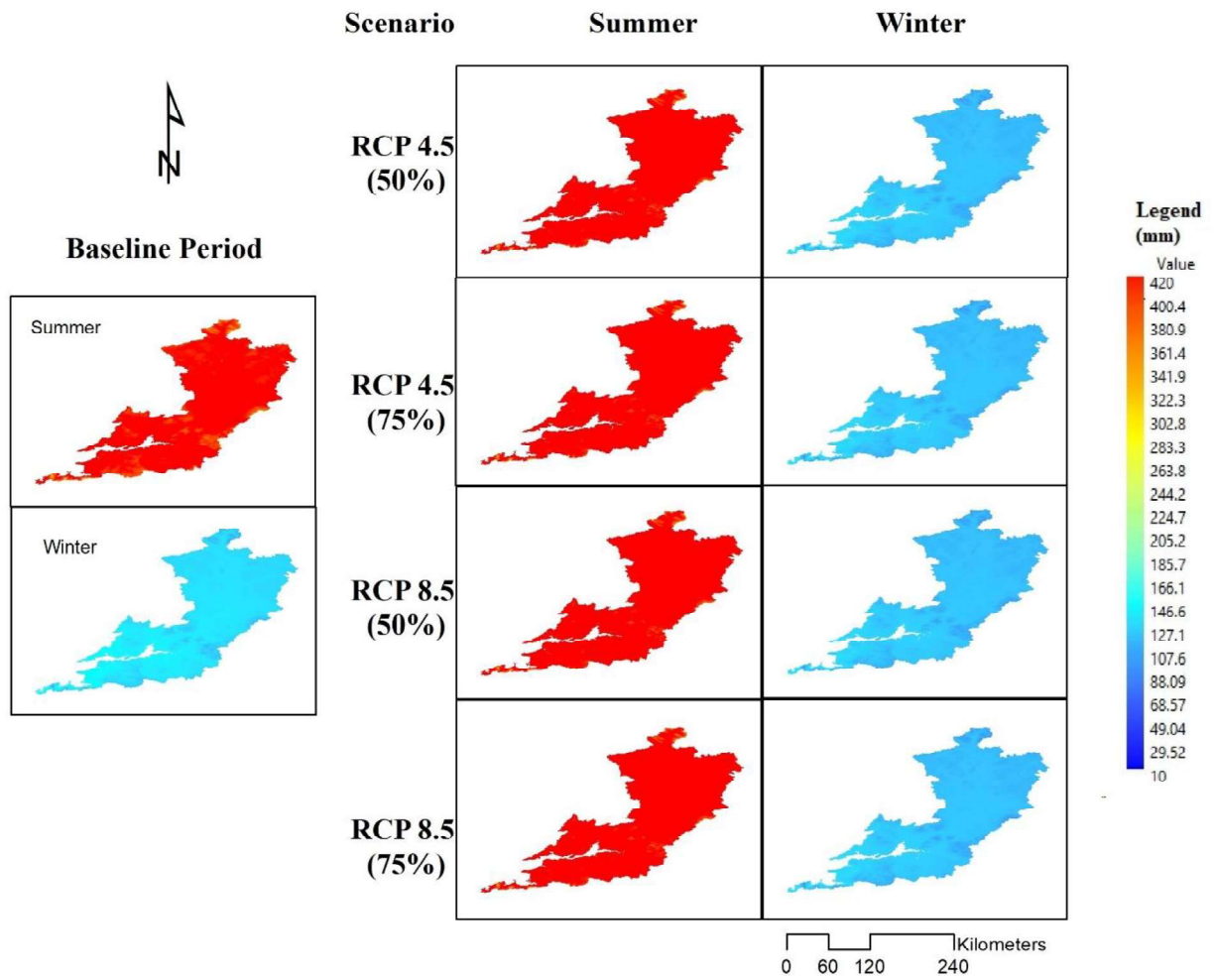
606 The Hamon method was first applied to mean monthly temperature data from 2020 for the four  
 607 modeled climate change scenarios. Given the uncertainty of future climate change, monthly PETS  
 608 raster maps were aggregated to represent growing (April to September) and non-growing (October to  
 609 March) seasons, herein termed summer and winter respectively. Seasonal raster maps for baseline and  
 610 2020 PETS projections are presented in Figure 18. As can be seen, a summer and winter raster map  
 611 were created for each scenario. In order to evaluate the effect of climate change on PETS under the  
 612 scenarios considered, seasonal PETS values at the same four locations as previously have been  
 613 compared with baseline values as shown in Table 3.

614

615 **Table 3: Seasonal PETS Baseline and projections for 2020 at four synoptic stations located in**  
 616 **the Shannon River Basin District.**

Location	Baseline		50% Delta RCP4.5		50% Delta RCP8.5		75% Delta RCP4.5		75% Delta RCP8.5	
	Winter	Summer	Winter	Summer	Winter	Summer	Winter	Summer	Winter	Summer
<b>Mullingar (Sy.S.1)</b>	116.5	434.7	117.6	439.0	117.8	439.8	117.8	439.0	118.1	440.6
<b>Mount Dillon (Sy.S.2)</b>	118.6	442.1	119.6	446.0	119.8	446.7	119.8	446.0	120.0	447.8
<b>Gurteen College (Sy.S.3)</b>	121.2	446.3	122.2	450.6	122.4	451.1	122.4	450.6	122.7	452.3
<b>Shannon Airport (Sy.S.4)</b>	127.8	470.2	128.9	474.3	129.1	475.0	129.2	474.3	129.4	476.4
<b>Mean</b>	121.0	448.3	122.1	452.5	122.3	453.2	122.3	452.5	122.6	454.3
<b>% Change</b>			0.9	0.9	1.0	1.1	1.1	0.9	1.3	1.3

617



618

619

**Figure 18: Seasonal PETS baseline and projections for 2020 according to different**

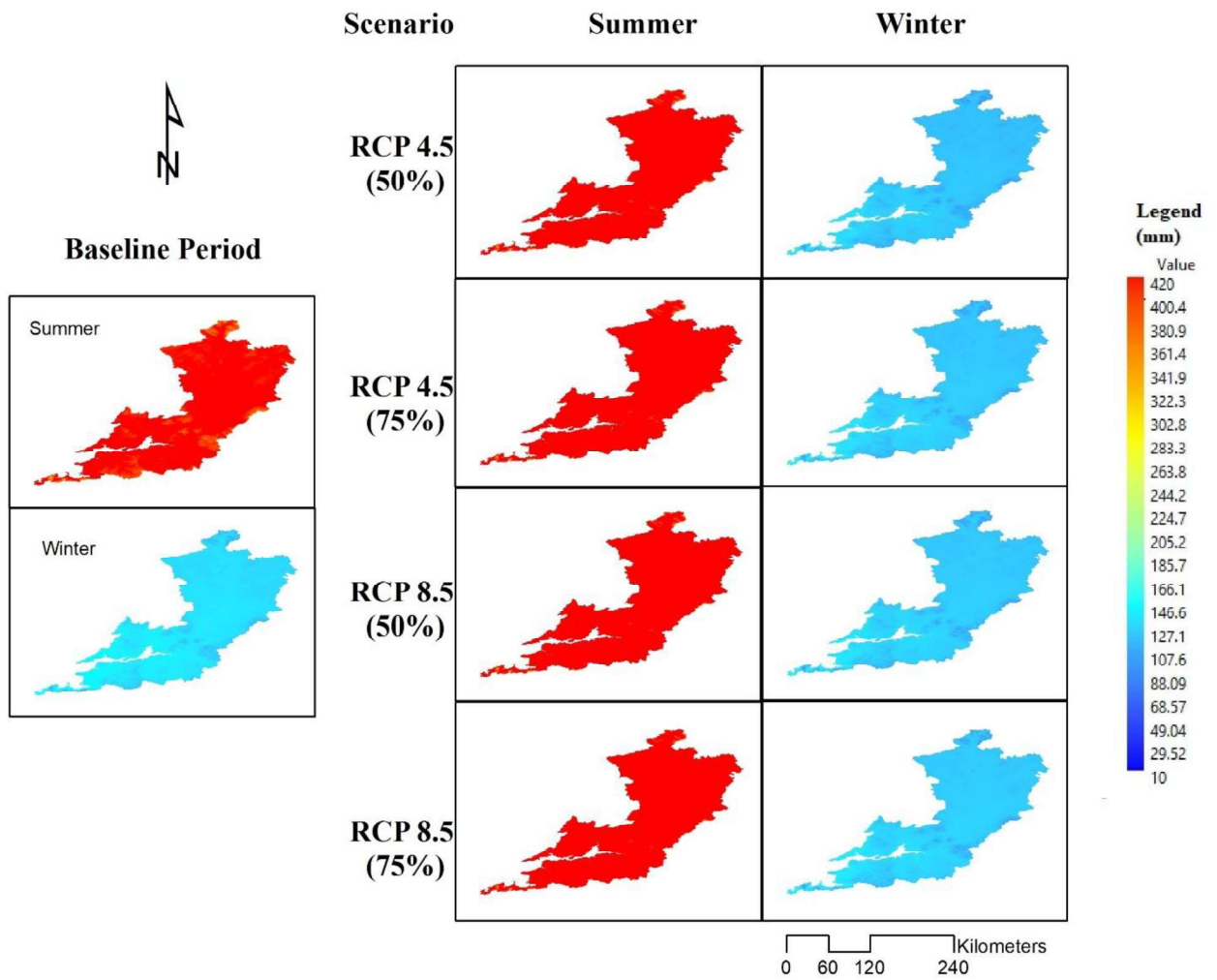
620

**Representative Concentration Pathways.**

621

622

Similarly, to 2020, results for 2050 are shown in Figure 19 and Table 4.



623

624

625

**Figure 19: Seasonal PETS baseline and projections for 2050 according to different Representative Concentration Pathways.**

626

627 **Table 4: Seasonal PETS Baseline and projections for 2050 at four synoptic stations located in**  
628 **the Shannon River Basin District.**

	Baseline		50% Delta RCP4.5		50% Delta RCP8.5		75% Delta RCP4.5		75% Delta RCP8.5	
	Winter	Summer	Winter	Summer	Winter	Summer	Winter	Summer	Winter	Summer
<b>Mullingar (Sy.S.1)</b>	116.5	434.7	120.5	452.0	122.6	460.5	121.3	450.7	123.8	464.9
<b>Mount Dillon (Sy.S.2)</b>	118.6	442.1	122.4	459.2	124.5	465.5	123.1	460.1	125.5	469.9
<b>Gurteen College (Sy.S.3)</b>	121.2	446.3	125.3	467.9	127.6	472.6	126.2	470.0	128.9	478.0
<b>Shannon Airport (Sy.S.4)</b>	127.8	470.2	132.0	474.8	134.3	494.2	132.9	486.8	135.6	496.0
<b>Mean</b>	121.0	448.3	125.1	463.5	127.3	473.2	125.9	466.9	128.5	477.2
<b>% Change</b>			3.3	3.4	5.1	5.5	4.0	4.1	6.1	6.4

629

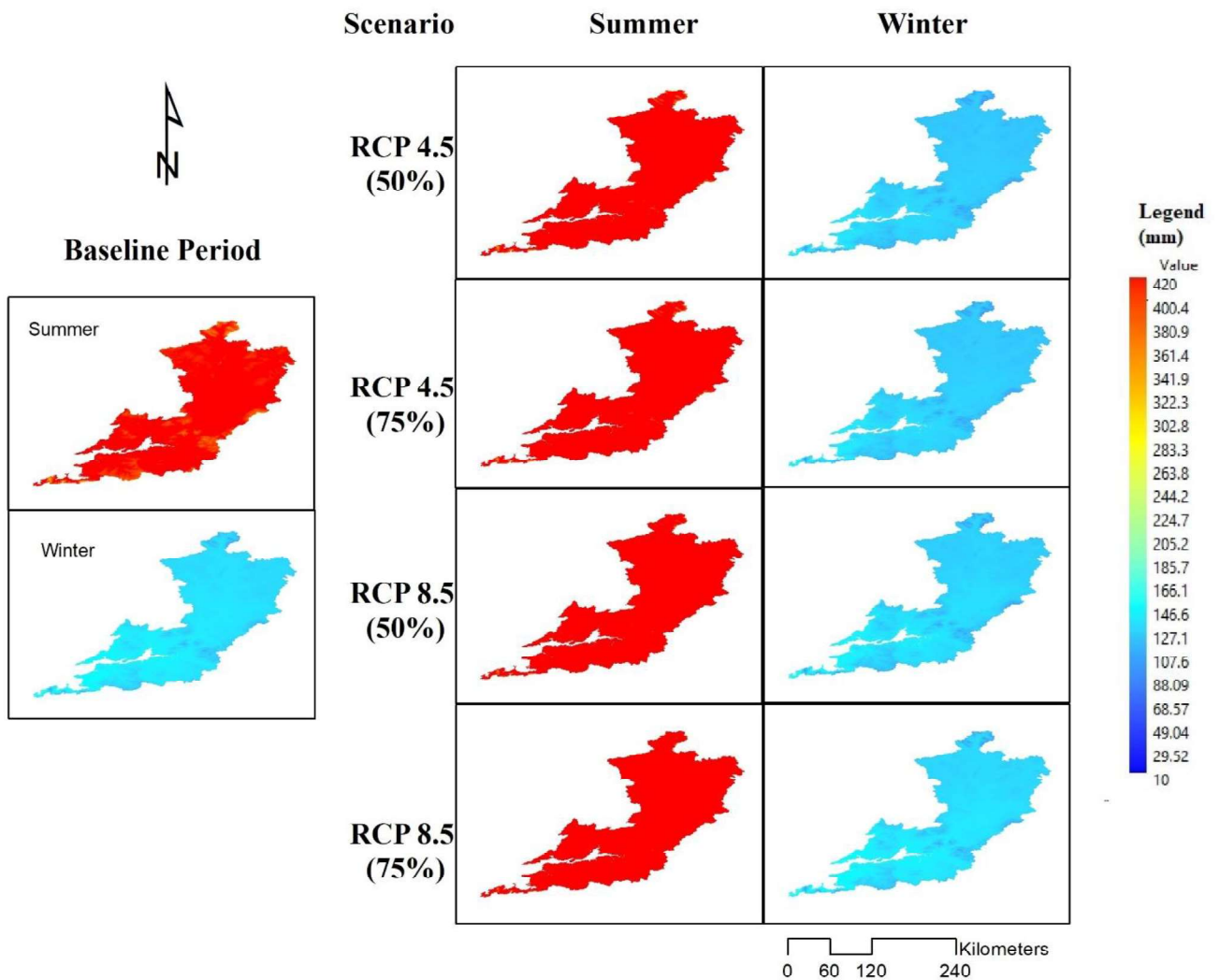
630 **Table 5: Seasonal PETS Baseline and projections for 2080 at four synoptic stations located in**  
631 **the Shannon River Basin District.**

	Baseline		50% Delta RCP4.5		50% Delta RCP8.5		75% Delta RCP4.5		75% Delta RCP8.5	
	Winter	Summer	Winter	Summer	Winter	Summer	Winter	Summer	Winter	Summer
<b>Mullingar (Sy.S.1)</b>	116.5	434.7	122.3	458.4	129.0	458.4	123.4	456.5	131.4	497.0
<b>Mount Dillon (Sy.S.2)</b>	118.6	442.1	124.2	463.5	130.7	463.5	125.2	466.0	132.9	500.9
<b>Gurteen College (Sy.S.3)</b>	121.2	446.3	127.2	470.1	134.5	470.1	128.5	477.2	137.3	510.1
<b>Shannon Airport (Sy.S.4)</b>	127.8	470.2	133.9	490.0	141.1	492.1	135.2	492.5	143.8	527.9
<b>Mean</b>	121.0	448.3	126.9	470.5	133.8	471.0	128.1	473.1	136.4	509.0
<b>% Change</b>			4.9	4.9	10.6	5.1	5.8	5.5	12.7	13.5

632

633

634 Finally, results for 2080 scenarios are presented in Figure 20 and Table 5.



635

636

**Figure 20: Seasonal PETS baseline and projections for 2080 according to different**

637

**Representative concentration pathways.**

638 The results present evidence that the modeled climate change scenarios would have a significant

639 impact on future PETS rates within the Shannon River Basin District. In all locations, all scenarios

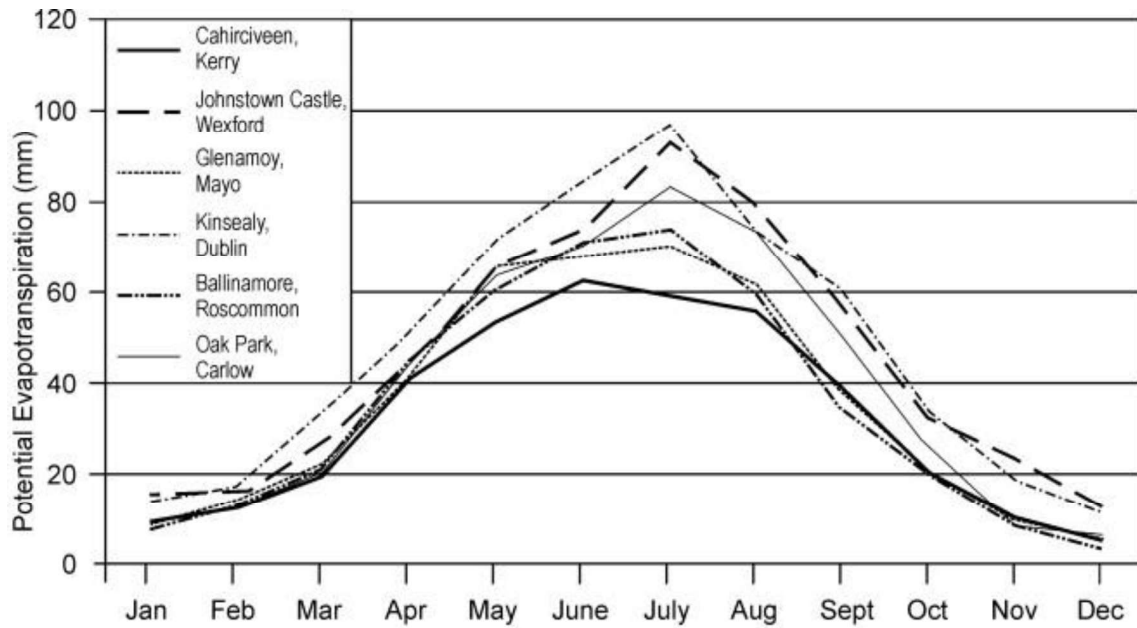
640 predicted an increase in PETS for each future time interval.

641

## 642 Discussion

643 Empirical PETS equations are most suited to the regions within which they are developed;  
644 consequently, one would expect disparity between results for different methods for given conditions.  
645 From the results, it can be seen that there exists significant deviation between modelled results of up  
646 to 61.9 mm per month (Blaney-Criddle/Hamon in July at Mount Dillon), which means that each  
647 method simulates statistically significant different results from the other methods and there were no  
648 single pair of methods that can produce statistically significant similar PETS estimates. Also, it can be  
649 seen that the Blaney-Criddle, Kharrufa, and Hargreaves and Samani methods consistently  
650 overestimate PETS and with their large mean RMSE values of 40.6 mm, 28.5 mm and 15.3 mm  
651 respectively, they were concluded as unsuitable for application within the Shannon River Basin  
652 District and excluded from further evaluation. As can be seen, the remaining three methods  
653 consistently returned relatively similar results and in addition, although the Penman-Monteith may be  
654 the most reliable method, the Met Éireann PETS values are also subject to error making it difficult to  
655 ascertain the most accurate model. Yoder et al. (2005) compared lysimeter data with the Penman-  
656 Monteith method in a wet/humid region in the south-eastern United States similar to conditions  
657 prevailing in Ireland and found an  $R^2$  of 0.91 with an error of 0.31 mm/day. Given this error it is  
658 possible to accumulate a total error of 9.3 mm in a 30 day period (Yoder et al., 2005). From Figures  
659 16-17, it can be seen the presence of such an error could have a significant impact on the relative  
660 accuracy of the Oudin, Thornthwaite and Hamon Methods. As can be seen, there exists a substantial  
661 spatial variation in PETS for a given period (in excess of 35 mm for July). Variations in excess of  
662 20 mm exist between Oak Park Co. Carlow and Johnstown Castle Co. Wexford for July, which are  
663 sited approximately 70 km apart, see Figure 1 for the locations. This represents approximately 33% of  
664 that measured at Oak Park. When Figure 21 is compared with Figure 17, it can be seen that values of  
665 PETS calculated using the Hamon method for all locations correlate reasonably well with the  
666 trends of measured values. While this does not validate the application of the Hamon method, it does  
667 demonstrate the capacity of the formula to reasonably account for variations in PETS within the Irish

668 climate.



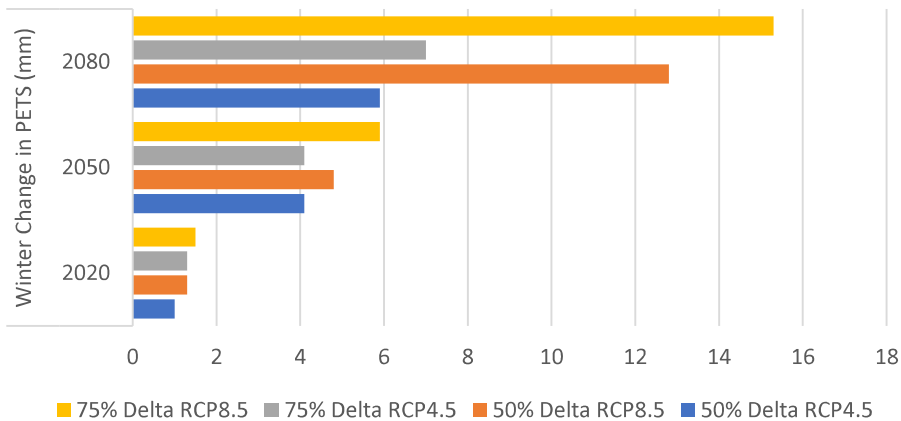
669

670 **Figure 21: Average monthly evapotranspiration measured at six lysimeters over the period**  
671 **1971-1990 (Mills, 2000).**

672 Throughout the last 50 years, the global climate has been subjected to warming because of the  
673 continuous rise in the concentration of greenhouse gasses in the atmosphere, which can be largely  
674 attributed to human activities (Stocker et al., 2013). Numerous studies of climate change have  
675 successfully revealed that the Earth's atmosphere is being altered by anthropogenic and biogenic  
676 emissions of carbon dioxide, other radioactively active gasses and aerosol precursors such as Sulphur  
677 dioxide (Chattopadhyay and Hulme, 1997). Global climate change is influencing the hydrological  
678 cycle by shifting rates of precipitation, recharge, discharge, and ET. To give an example of possible  
679 future scenarios; decreased precipitation during winter months to recharge groundwater storage within  
680 the Shannon River Basin District could exacerbate problems caused by reduced summer precipitation  
681 and increased ET rates. Consequently, reduced storage would result in less water being available  
682 during the drier summer months to sustain low flows and could result in water shortages. PETS was  
683 spatially modeled within the Shannon River Basin District for three future time intervals (2020, 2050  
684 and 2080) using the Hamon method. For each time interval, data from four climate change scenarios

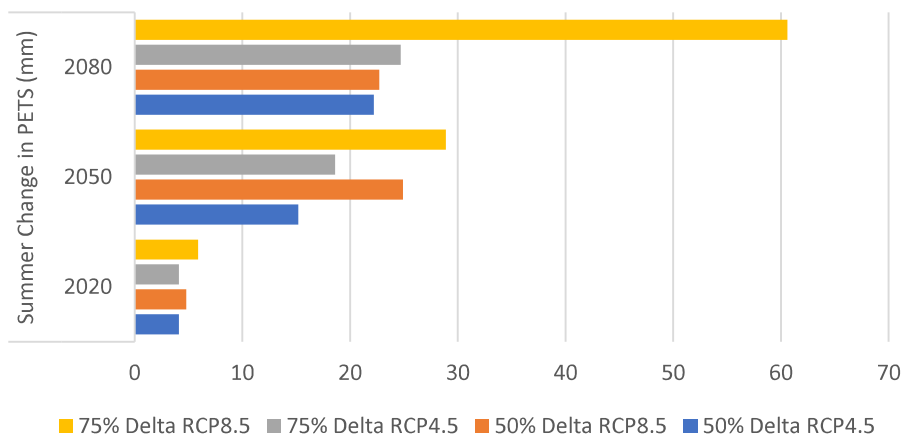
685 were modeled in an attempt to take consideration of the indefinite nature of future climate change. A  
686 clear trend is evident in the results, where PETS is continuously increasing as a result of climate  
687 change from 0.9%-1.3% in 2020 up to 13.5% in 2080. A similar trend was discovered by (Scheff and  
688 Frierson, 2014), who modeled the effect of the warming of the earth's climate as a result of  
689 greenhouse gas pollution on PETS over the 21st century and found that variations in annual- mean  
690 PETS over the upcoming century are almost always positive. In order to better illustrate the  
691 fluctuations found in this study, Figure 22 displays the mean seasonal deviation of PETS for each  
692 scenario considered. This figure further exhibits the increasing trend of PETS in the future, which  
693 may significantly affect water resources and availability in the Shannon River Basin District.

(A)



694

(B)



695

696

**Figure 22: Mean deviation of future seasonal PETS from baseline results for four climate change scenarios. (A) Winter season, (B) Summer season.**

697

698

### *Conclusions*

699

700

701

702

703

704

705

Evapotranspiration integrates energy and mass transfer between the Earth's surface and atmosphere and is the most active mechanism linking the atmosphere, hydrosphere, lithosphere and biosphere, it is responsible for monitoring atmospheric moisture and temperature. This study aimed to spatially estimate PETS, a complex hydrological process, within Ireland's Shannon River Basin District using GIS-based algorithms. The ability to accurately determine PETS is of critical importance in resource evaluation and sustainable water resource management policies as well as a host of hydrological and agricultural studies. Because of its complexity, and inherent spatial

706 variability, PETS is particularly difficult to determine for a given location. From the selection of  
707 possible approaches, the use of empirical PETS formulae which integrate empirical constants and  
708 meteorological data were selected as the most appropriate method. Compared to more complex  
709 methods these relatively simple formulae require data which is monitored at a greater number of  
710 locations within the region, thus providing a more reliable spatial distribution of data. For example,  
711 temperature data which was used in this study was taken from 96 monitoring stations whereas more  
712 complex methods would require a host of variables some of which may only be measured at the  
713 four synoptic weather stations within the region or not at all. In this study, based on the availability  
714 of data, the complexity of formulae and their appropriateness for application within a GIS a number  
715 of methods were shortlisted.

716 Six temperature based methods were selected which would allow for the most appropriate to be  
717 identified. The 6 selected methods were applied within a GIS and each successfully produced long-  
718 term mean monthly PETS raster maps of the region. Through comparison with the Met Éireann  
719 data, the Hamon method was found to produce the most precise results with an RMSE of 8.6 mm.  
720 Each method applied in its own produced spatially distributed estimates of PETS. However, the  
721 Hamon method given its comparability to Met Éireann values and PETS trends was determined to be  
722 the most appropriate of the models tested and concluded to produce reasonable estimates of PETS  
723 within the Shannon River Basin District. It could be concluded that Hamon method was performing  
724 the best for the Shannon catchment because of the simple parameterization which includes two main  
725 factors, the daytime period and the temperature, with an exponential relation which is one of the main  
726 deference between Hamon and the other methods.

727 The Hamon method was therefore applied for three future time intervals (2020, 2050 and 2080) to  
728 study the effects of climate change. Four possible climate change scenarios were considered and  
729 associated future temperature for these scenarios was available through the downscaling results from  
730 (Gharbia et al., 2016b). The results present evidence that the modeled climate change scenarios would  
731 have a significant impact on future PETS rates within the Shannon River Basin District. In all  
732 locations, all scenarios predicted an increase in PETS for each future time interval. The scale of

733 increases in PETS was found to vary depending on climate change scenario and year. The  
734 maximum mean increase in PETS was as a result of the 75% RCP 8.5 scenario in 2080 which  
735 returned an increase of 75.9 mm annually. A clear trend is evident in in this study, where PETS is  
736 continuously increasing as a result of climate change from 0.9%-1.3% in 2020 up to 13.5% in 2080.  
737 The calculated mean seasonal deviations of projected PETS from the baseline have significantly show  
738 the increase in the PETS rates and trends for each scenario considered, which may significantly affect  
739 water resources and availability in the Shannon River Basin District. For future related research, the  
740 same process and algorithms should be applied on other catchments in different climatic zones which  
741 allows the validate the process in the different climates.

742

### 743 Acknowledgments

744 This research was funded jointly by Trinity College, Dublin through the Postgraduate Ussher  
745 Fellowship Award and by iSCAPE (Improving Smart Control of Air Pollution in Europe) project,  
746 which is funded by the European Community's H2020 Programme (H2020-SC5-04-2015) under the  
747 Grant Agreement No. 689954.

### 748 References

- 749 ABTEW, W. 1996. Evapotranspiration measurements and modeling for three wetland systems in  
750 south florida1. Wiley Online Library.
- 751 ALLEN, R. G. 2000. Using the FAO-56 dual crop coefficient method over an irrigated region as part  
752 of an evapotranspiration intercomparison study. *Journal of Hydrology*, 229, 27-41.
- 753 ALLEN, R. G., PEREIRA, L. S., RAES, D. & SMITH, M. 1998. Crop evapotranspiration-Guidelines  
754 for computing crop water requirements-FAO Irrigation and drainage paper 56. *FAO, Rome*,  
755 300, D05109.
- 756 ALLEN, R. G. & PRUITT, W. O. 1986. Rational use of the FAO Blaney-Criddle formula. *Journal of*  
757 *Irrigation and Drainage Engineering*, 112, 139-155.

758 ANDRÉASSIAN, V. 2004. Waters and forests: from historical controversy to scientific debate.  
759 *Journal of Hydrology*, 291, 1-27.

760 ANDRÉASSIAN, V., PERRIN, C. & MICHEL, C. 2004. Impact of imperfect potential  
761 evapotranspiration knowledge on the efficiency and parameters of watershed models. *Journal*  
762 *of Hydrology*, 286, 19-35.

763 BLANEY, H. F. & CRIDDLE, W. D. 1964. Determining water requirements for settling water  
764 disputes. *Nat. Resources J.*, 4, 29.

765 CHATTOPADHYAY, N. & HULME, M. 1997. Evaporation and potential evapotranspiration in India  
766 under conditions of recent and future climate change. *Agricultural and Forest Meteorology*,  
767 87, 55-73.

768 CHOAT, B., JANSEN, S., BRODRIBB, T. J., COCHARD, H., DELZON, S., BHASKAR, R.,  
769 BUCCI, S. J., FEILD, T. S., GLEASON, S. M. & HACKE, U. G. 2012. Global convergence  
770 in the vulnerability of forests to drought. *Nature*, 491, 752-755.

771 DE BRUIN, H. 1983. A model for the Priestley-Taylor parameter  $\alpha$ . *Journal of climate and applied*  
772 *meteorology*, 22, 572-578.

773 DROOGERS, P. & ALLEN, R. G. 2002. Estimating reference evapotranspiration under inaccurate  
774 data conditions. *Irrigation and drainage systems*, 16, 33-45.

775 FENNESSEY, N. M. & VOGEL, R. M. 1996. Regional models of potential evaporation and reference  
776 evapotranspiration for the northeast USA. *Journal of Hydrology*, 184, 337-354.

777 GHARBIA, S. S., ALFATAH, S. A., GILL, L., JOHNSTON, P. & PILLA, F. 2016a. Land use  
778 scenarios and projections simulation using an integrated GIS cellular automata algorithms.  
779 *Modeling Earth Systems and Environment*, 2, 151.

780 GHARBIA, S. S., GILL, L., JOHNSTON, P. & PILLA, F. GEO-CWB: a Dynamic Water Balance  
781 Tool for Catchment Water Management. 5th International Multidisciplinary Conference on  
782 Hydrology and Ecology (HydroEco2015), At Vienna, Austria, 2015a.

783 GHARBIA, S. S., GILL, L., JOHNSTON, P. & PILLA, F. Trans-boundary European River's Long-  
784 term Changes Analysis for Water Level and Streamflow Regime. 42nd IAH Congress  
785 (AQUA2015), At Rome, Italy, 2015b.

786 GHARBIA, S. S., GILL, L., JOHNSTON, P. & PILLA, F. 2016b. Multi-GCM ensembles  
787 performance for climate projection on a GIS platform. *Modeling Earth Systems and*  
788 *Environment*, 2, 1-21.

789 GHARBIA, S. S., GILL, L., JOHNSTON, P. & PILLA, F. 2016c. Using GIS Based Algorithms for  
790 GCMs' Performance Evaluation. *18th IEEE Mediterranean Electrotechnical Conference*  
791 *MELECON 2016*. Cyprus: IEEE.

792 GHARBIA, S. S., JOHNSTON, P., GILL, L. & PILLA, F. 2016d. Using GIS Based Algorithms for  
793 GCMs' Performance Evaluation. *strategies*, 2, 3.

794 GORDON, D. R. 1998. Effects of invasive, non-indigenous plant species on ecosystem processes:  
795 lessons from Florida. *Ecological Applications*, 8, 975-989.

796 HAMON, W. R. 1961. Estimating potential evapotranspiration. *Journal of the Hydraulics Division*,  
797 87, 107-120.

798 HARGREAVES, G. H. & SAMANI, Z. A. 1982. Estimating potential evapotranspiration. *Journal of*  
799 *the Irrigation and Drainage Division*, 108, 225-230.

800 HARGREAVES, G. H. & SAMANI, Z. A. 1985. Reference crop evapotranspiration from  
801 temperature. *Applied engineering in agriculture*, 1, 96-99.

802 HOLDRIDGE, L. R. 1959. Simple method for determining potential evapotranspiration from  
803 temperature data. *Science*, 130, 572-572.

804 HOLLAND, W. R. 1978. The role of mesoscale eddies in the general circulation of the ocean-  
805 numerical experiments using a wind-driven quasi-geostrophic model. *Journal of Physical*  
806 *Oceanography*, 8, 363-392.

807 JENSEN, M. E., BURMAN, R. D. & ALLEN, R. G. Evapotranspiration and irrigation water  
808 requirements. 1990. ASCE.

809 KAY, A. & DAVIES, H. 2008. Calculating potential evaporation from climate model data: a source  
810 of uncertainty for hydrological climate change impacts. *Journal of Hydrology*, 358, 221-239.

811 KHARRUFA, N. 1985. Simplified equation for evapotranspiration in arid regions. *Beiträge zur*  
812 *Hydrologie*, 5, 39-47.

813 KITE, G. W. & DROOGERS, P. 2000. Comparing evapotranspiration estimates from satellites,  
814 hydrological models and field data. *Journal of Hydrology*, 229, 3-18.

815 LINACRE, E. T. 1977. A simple formula for estimating evaporation rates in various climates, using  
816 temperature data alone. *Agricultural meteorology*, 18, 409-424.

817 LIU, Y. & PHINN, S. R. 2003. Modelling urban development with cellular automata incorporating  
818 fuzzy-set approaches. *Computers, Environment and Urban Systems*, 27, 637-658.

819 MAKKINK, G. 1957. Testing the Penman formula by means of lysimeters. *J. Inst. Water Eng*, 11,  
820 277-288.

821 MCGUINNESS, J. L. & BORDNE, E. F. 1972. *A comparison of lysimeter-derived potential*  
822 *evapotranspiration with computed values*, US Dept. of Agriculture.

823 MILLS, G. 2000. Modelling the water budget of Ireland—evapotranspiration and soil moisture. *Irish*  
824 *Geography*, 33, 99-116.

825 OUDIN, L., HERVIEU, F., MICHEL, C., PERRIN, C., ANDRÉASSIAN, V., ANCTIL, F. &  
826 LOUMAGNE, C. 2005. Which potential evapotranspiration input for a lumped rainfall–  
827 runoff model?: Part 2—Towards a simple and efficient potential evapotranspiration model for  
828 rainfall–runoff modelling. *Journal of Hydrology*, 303, 290-306.

829 OUDIN, L., MOULIN, L., BENDJOUDI, H. & RIBSTEIN, P. 2010. Estimating potential  
830 evapotranspiration without continuous daily data: possible errors and impact on water balance  
831 simulations. *Hydrological Sciences Journal–Journal des Sciences Hydrologiques*, 55, 209-  
832 222.

833 PARMELE, L. & MCGUINNESS, J. 1974. Comparisons of measured and estimated daily potential  
834 evapotranspiration in a humid region. *Journal of Hydrology*, 22, 239-251.

835 PENMAN, H. L. Natural evaporation from open water, bare soil and grass. Proceedings of the Royal  
836 Society of London A: Mathematical, Physical and Engineering Sciences, 1948. The Royal  
837 Society, 120-145.

838 PORTUGALI, J., IZAK, B. & IZAK, O. 1994. *Geographical Analysis*, 26, 321.

839 PRUITT, W. & DOORENBOS, J. 1977. *Empirical Calibration: A Requisite for Evapotranspiration*  
840 *Formulae Based on Daily Or Longer Mean Climate Data?*, The Committee.

841 ROMANENKO, P. 1973. Effect of a Transverse Mass Flow on Heat Transfer and Dynamics of a  
842 Turbulent Hot Air Flow in Axi Symmetric Diffusor with a Permeable Wall. DTIC Document.

843 ROSENZWEIG, M. L. 1968. Net primary productivity of terrestrial communities: prediction from  
844 climatological data. *American Naturalist*, 67-74.

845 SCHEFF, J. & FRIERSON, D. M. 2014. Scaling potential evapotranspiration with greenhouse  
846 warming. *Journal of Climate*, 27, 1539-1558.

847 SHUKLA, J. & MINTZ, Y. 1982. Influence of land-surface evapotranspiration on the earth's climate.  
848 *Science*, 215, 1498-1501.

849 SINGH, V. & XU, C. 1997. Evaluation and generalization of 13 mass-transfer equations for  
850 determining free water evaporation. *Hydrological processes*, 11, 311-323.

851 STOCKER, T. F., QIN, D., PLATTNER, G., TIGNOR, M., ALLEN, S., BOSCHUNG, J., NAUELS,  
852 A., XIA, Y., BEX, V. & MIDGLEY, P. 2013. Climate change 2013: the physical science  
853 basis. Intergovernmental panel on climate change, working group I contribution to the IPCC  
854 fifth assessment report (AR5). New York: Cambridge University Press.

855 SWENSON, S. & WAHR, J. 2006. Estimating large-scale precipitation minus evapotranspiration  
856 from GRACE satellite gravity measurements. *Journal of Hydrometeorology*, 7, 252-270.

857 THORNTHWAITE, C. W. 1948. An approach toward a rational classification of climate.  
858 *Geographical review*, 38, 55-94.

859 THORNTHWAITE, C. W. & MATHER, J. R. 1957. Instructions and tables for computing potential  
860 evapotranspiration and the water balance.

- 861 TURC, L. 1961. Estimation of irrigation water requirements, potential evapotranspiration: a simple  
862 climatic formula evolved up to date. *Ann Agron*, 12, 13-49.
- 863 WILSON, K. B., HANSON, P. J., MULHOLLAND, P. J., BALDOCCHI, D. D. &  
864 WULLSCHLEGER, S. D. 2001. A comparison of methods for determining forest  
865 evapotranspiration and its components: sap-flow, soil water budget, eddy covariance and  
866 catchment water balance. *Agricultural and forest Meteorology*, 106, 153-168.
- 867 WU, F. 2002. Calibration of stochastic cellular automata: the application to rural-urban land  
868 conversions. *International Journal of Geographical Information Science*, 16, 795-818.
- 869 XU, C.-Y. & SINGH, V. 2002. Cross comparison of empirical equations for calculating potential  
870 evapotranspiration with data from Switzerland. *Water Resources Management*, 16, 197-219.
- 871 XU, C. & SINGH, V. 2000. Evaluation and generalization of radiation-based methods for calculating  
872 evaporation. *Hydrological processes*, 14, 339-349.
- 873 XU, C. Y. & SINGH, V. 2001. Evaluation and generalization of temperature- based methods for  
874 calculating evaporation. *Hydrological processes*, 15, 305-319.
- 875 YODER, R., ODHIAMBO, L. & WRIGHT, W. 2005. Evaluation of methods for estimating daily  
876 reference crop evapotranspiration at a site in the humid southeast United States. *Applied  
877 engineering in agriculture*, 21, 197-202.
- 878 ZHANG, L., DAWES, W. & WALKER, G. 2001. Response of mean annual evapotranspiration to  
879 vegetation changes at catchment scale. *Water Resources Research*, 37, 701-708.
- 880 ZHAO, C., FENG, Z. & CHEN, G. 2004. Soil water balance simulation of alfalfa (*Medicago sativa*  
881 L.) in the semiarid Chinese Loess Plateau. *Agricultural water management*, 69, 101-114.

882